Copyright Warning & Restrictions

The copyright law of the United States (Title 17, United States Code) governs the making of photocopies or other reproductions of copyrighted material.

Under certain conditions specified in the law, libraries and archives are authorized to furnish a photocopy or other reproduction. One of these specified conditions is that the photocopy or reproduction is not to be "used for any purpose other than private study, scholarship, or research." If a, user makes a request for, or later uses, a photocopy or reproduction for purposes in excess of "fair use" that user may be liable for copyright infringement,

This institution reserves the right to refuse to accept a copying order if, in its judgment, fulfillment of the order would involve violation of copyright law.

Please Note: The author retains the copyright while the New Jersey Institute of Technology reserves the right to distribute this thesis or dissertation

Printing note: If you do not wish to print this page, then select "Pages from: first page # to: last page #" on the print dialog screen

ABSTRACT

AN ANALYSIS OF THE PERIODICITY OF THE CELL CYCLE AND APOPTOTIC REGULATORY PROTEINS IN PROSTATE XENOGRAFTS USING ANOVA AND COSINOR METHODS

by
Aleen Hosdaghian

Circadian rhythms have been found in both plants and animals, in normal tissues as well as in most tumors and human cancers. By following these rhythms in healthy and cancerous tissue, it has been possible to find optimal times to deliver a dose of drug, such that efficacy is maximized and toxicity to normal tissues is minimized. In this study, the periodicity of several cell cycle and apoptotic regulatory proteins were studied in two prostate cancer models against a dietary therapeutic agent, Selenium. The ALVA-31 (androgen-independent) and PC-3 (androgen-independent) prostate cancer cell lines were grown *in vivo*, as a subcutaneous xenograft in mice and measured at seven different **H**ours **A**fter **L**ight **O**nset (HALO). Measurements were taken at 3, 7, 10, 13, 17, 20 and 23 HALO, which is equivalent to 10 AM, 1 PM, 4 PM, 7 PM, 11 PM, 2 AM and 5 AM. The tumors were used to assess total expression of the protein of interest using an immunoblotting method, and the results were assessed by densitometry. Statistical analysis of the mice with the ANOVA and the COSINOR methods showed that selenium treatment was most effective at HALO 13 at decreasing cell cycle and apoptosis-related proteins for ALVA-31. For PC-3 tumor lines, HALO 7 proved to be of highest expression while HALO 13 showed the lowest expression. The selenium treated tumors showed inhibitory effects via lower expression levels throughout both tumor trials.

AN ANALYSIS OF THE PERIODICITY OF THE CELL CYCLE AND APOPTOTIC REGULATORY PROTEINS IN PROSTATE XENOGRAFTS USING ANOVA AND COSINOR METHODS

by
Aleen Hosdaghian

A Thesis
Submitted to the Faculty of
New Jersey Institute of Technology and
Rutgers, The State University of New Jersey - Newark
in Partial Fulfillment of the Requirements for the Degree of
Master of Science in Computational Biology

Federated Biological Sciences Department

January 2004

APPROVAL PAGE

AN ANALYSIS OF THE PERIODICITY OF THE CELL CYCLE AND APOPTOTIC REGULATORY PROTEINS IN PROSTATE XENOGRAFTS USING ANOVA AND COSINOR METHODS

Aleen Hosdaghian

Dr. Michael Recce, Thesis Co-Advisor — Date
Director, Life Sciences Program and Center for Computational Biology
New Jersey Institute of Technology

Dr. Rosalyn Blumenthal, Thesis Co-Advisor — Date
Director, Tumor Biology
Garden State Cancer Center

Dr. Zaven Ariyan, Committee Member — Date
Adjunct Professor, Medicinal Chemistry
New Jersey Institute of Technology

BIOGRAPHICAL SKETCH

Author: Aleen Hosdaghian

Degree: Master of Science

Date: January 2004

Education:

- Master of Science in Computational Biology,
  New Jersey Institute of Technology, Newark, NJ, 2004

- Bachelor of Science in Biology,
  State University of New York at Cortland, Cortland, NY, 1999

Major: Computational Biology

To my parents Garabed and Sosi Hosdaghian for their unconditional support and love, and to my brother Shaunt who always reminds me to laugh.

Seterak G. Hosdaghian
In memoriam

ACKNOWLEDGMENT

I would like to thank Dr. Michael Recce for his advisement and leadership for my thesis and throughout the entire computational biology program at NJIT. Also, I would like to thank Dr. Rosalyn Blumenthal for serving as co-advisor and for the opportunity to perform my study at the Garden State Cancer Center and whose support made this thesis possible. I would like to express my gratitude to Dr. Zaven Ariyan for offering his expertise and agreeing to be a part of my thesis committee.

Thanks to all employees of the Garden State Cancer Center for their invaluable guidance and resources.

A special thanks to Ali Nasab who has given his insight, resources, and continual motivation from the conception to the completion of this thesis.

TABLE OF CONTENTS

LIST OF TABLES

LIST OF FIGURES

LIST OF FIGURES
(Continued)

CHAPTER 1

INTRODUCTION

The phase of cell cycle and apoptosis plays a critical role in chemosensitivity in cancer. In this study, chronotherapy studies with human prostate cancer cell lines ALVA-31 and PC-3 were used to determine the expression patterns of various cell cycle and apoptosis regulatory proteins. Expression patterns were also studied using the dietary treatment Selenium in the form of Sodium Selenite. The prostate tumor cell lines were grown as subcutaneous xenografts in mice and their periodicity of expression compared to the periodicity of normal tissue of lung and kidney. Results were assessed by a comparison of the ANOVA and COSINOR methods.

1.1 Prostate Cancer

Prostate cancer is the most common cancer found in men in the United States. It was diagnosed in an estimated 189,000 US men and led to the death of over 30,200 in 2002 (Pienta 2002). Prostate cancer may be diagnosed by means of tissue biopsy, however, there is no universally agreed-upon strategic plan for its treatment nor for its management. Individual chemotherapeutic agents for the majority of tumors have not increased cure rates in cancer treatment (Shah 2001). In light of this, treatment of prostate cancer increasingly involves approaches that combine local therapies directed at the primary tumor together with systemic therapies to potentiate their effect and to control subclinical metastatic disease. Therapies usually range with the stage of the cancer and may include: monotherapy, minimal and maximal androgen blockade options, radiotherapy, adjuvant therapy, and herbal treatment.

Monotherapy is a common method of prostate cancer treatment. Monotherapy can include chemotherapy or prescription drug treatment including anti-hormone therapy, which interferes with the body's ability to make testosterone. Agents used include diethylstilbestrol (Stilphostrol®), goserelin (Zoladex®), leuprolide (Lupron®), flutamide (Eulexin®), bicalutamide (Casodex®), and ketoconazole (Nizoral®) (Healthnotes 2002). Though the treatments cannot cure prostate cancer, they often slow the cancer's growth and reduce the tumor size.

Minimal (Intermittent) and maximal androgen blockade options can be accomplished using a variety of methods. The common methods used for primary androgen withdrawal are bilateral orchiectomy, estrogen therapy, luteinizing hormone-releasing hormone (**LHRH**) analog, and antiandrogens (Leewansangtong 1998). Intermittent androgen suppression (**IAS**) involves a hormonal therapy for a limited amount of time until the patient shows a predetermined response. This may vary per individual but usually is associated with Prostate Specific Antigen (PSA) levels or prostate cancer symptom improvement. Once this is achieved, the therapy is discontinued until there is a sign of cancer progression. Applying the IAS method can include the administration of a single hormonal drug (such as an LHRH analog) or a combination of hormonal drugs (such as an LHRH analog and antiandrogen). There is no data to show the long-term effectiveness of IAS, and this type of therapy is still considered investigational (NCI 2002).

Radiotherapy can be one of many different procedures such as beams, permanent, and temporary implants (Brachytherapy), all with varying dosage. Radiotherapy traditionally includes the entire prostate, and sometimes the pelvic lymph nodes (Pienta

2002). A recent study suggests that treating the lymph nodes may help patients at risk for lymph node metastases. (Zaida et al., 1999). Brachytherapy for prostate cancer has been delivered using temporary high-dose-rate devices in patients with locally advanced disease (Pienta 2002). Long-term effects of this treatment are yet unclear. In patients with aggressive T2 clinically localized prostate cancer, surgical removal of the prostate (radical prostatectomy) may improve long-term survival (Pienta 2002).

Adjuvant therapy is a combination of various therapies with a goal of having an overall increased recovery rate. Adjuvant therapy can be used with chemotherapy, hormonal therapy, or radiation therapy can also be applied to add to the effectiveness of surgery or radiation in preventing recurrence of the disease (Pienta 2002). Studies have even examined the use of products such as PC-SPES, a combination of eight herbs in one capsule, each with an anti-tumor effect. However, PC-SPES has recently been removed from the market for containing Diethylstibestrol, (DES) a prescription estrogen medication that is known to be effective in treating prostate cancer (Meyer et al., 2002).

1.2 Human Prostate Tumor Models

The cells of the prostate gland normally only grow and divide in the presence of male hormones called androgens. Androgens and growth factors control the proliferation of normal and cancerous cells. The same is true for cancerous cells. There are three known AR gene polymorphisms: the "CAG" trinucleotide repeat, the "GGC" trinucleotide repeat, and the R726L single nucleotide polymorphism (CDC 2003). Mainly, treatments are used that block the affect of androgens and other growth factors to ultimately stop the cells from dividing. In advanced prostate cancer, the cells are able to grow and divide

without androgens and the blocking drugs have no affect on cancer growth. Dihydrotestosterone (**DHT**) is necessary for initial growth of prostate cancer cells. It functions by activation of the androgen receptor. Therapy of metastatic prostate cancer is based on blockade of androgen receptor function by androgen depletion and by antagonists (antiandrogens). Unfortunately, even following initial remission, the tumor retains its ability to grow, and can lead to a relapse. In many tumors the androgen receptor is still expressed and seems functionally active, even thought DHT is seemingly absent or the androgen receptor is apparently blocked. In other tumors, the androgen receptor pathway seems to be bypassed by other mechanisms of regulation of cell growth and cell survival (CDC 2003).

Some prostatic cancer cell lines have shown resistance to therapy. This may be because of protein expression such as HCP (not expressed in JCA1) or Bcl-2, Bax and p53. With cycloheximide treatment, Fas-resistant cell lines can be converted to Fas-sensitive cell lines. This intrinsic propensity to undergo Fas-mediated apoptosis could be a target for therapeutic intervention in androgen-independent metastatic prostate cancer. (Oskar 1997). Methods to overcome resistance have proven to be one of the many challenges in developing cancer therapeutics.

Alterations of the receptors for these factors might disrupt the growth regulations that lead to cancer formation (Harris 1992). Among growth factor receptors, the most frequently implicated in human cancer have been members of the class I receptor tyrosine kinase family, the epidermal growth factor (**EGF**) receptor family. This receptor family includes the EGF receptor (**EGFR, erbB1**), HER2/Neu (**erbB2**), erbB3, and erbB4 proteins (Kwong 1998).

In order to study prostate cancer, several models have been studied and established. Mainly rodent models were used in order to study tumors and their effects. Some of the different model types are discussed below. One type of model studied is a xenograft model. This is where human prostate tissue is transplanted into an animal in order to test aspects *in vivo*. There can be models of transgenic mice that express a certain antigen, for example, an SV40 T-antigen. A promoter that shows gene expression in prostate tissue can then control these antigens (NCI 2003). Another model type that may be used is a Syngraft, in which tissue (i.e. prostate precursor) from rodent embryos is isolated, transfected with oncogenes, and then implanted into an adult host (NCI 2003). Still yet, there may be rat models, which are hormonally induced susceptible to prostate cancer following treatment with androgens, estrogens, and carcinogenic agents, either alone or in combination. There exists a dog model, which spontaneously develops prostate cancer as a high incidence of prostatic intraepithelial neoplasia (PIN). The *in vitro* cell models, may be derived from prostate cancers and which have maintained phenotypic characteristics of the tumor, and finally, *in silico* computer models, which can mimic the proliferation of prostate tumors (NCI 2003).

Without a cure, scientists work mainly to achieve the goals of identifying and monitoring levels of Prostate Specific Antigen (**PSA**) for detection and providing therapies with lower thresholds of toxicity in hopes of reducing pain, and improving the quality of life. Chronotherapy is an area of research that may help to attain these goals. By mapping out the expression of proteins involved in cell cycle and apoptosis, one could identify the points that tumor genes interact and intercede to block proliferation at a point during the cell cycle or induce apoptosis of tumor cells by studying key apoptosis

proteins. The two tumor carcinoma cell lines used in this study were ALVA-31 and PC-3. Figure 1.1 shows the cell lines as they were grown in labs at UCLA. The cells were grown in this manner to ensure promotion of specific cell membrane associated adhesion within each other (UCLA 2003).

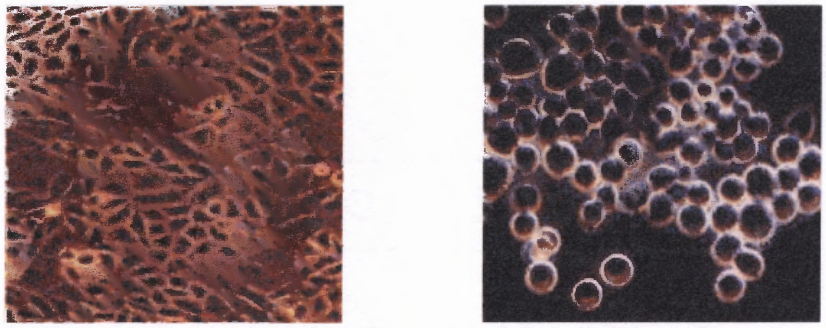

Figure 1.1 Representations of ALVA-31 and PC-3 cell lines. Grown in UCLA as 3 dimensional spheroid cells grown without adherence to any plastic surfaces.

1.3 Cell Cycle and Apoptosis in Prostate Cancer

When administering a therapeutic agent to a patient, many issues must be taken into account, aside from adversity to therapeutics, developing resistance is a concern. Cell cycle and apoptosis regulation may be key factors in determining the efficacy of a therapeutic agent. The cell cycle is the mechanism by which cells divide. It consists of four general phases including: G1 (growth and preparation of the chromosomes for replication), S (DNA synthesis), G2 (preparation for mitosis), and M (mitosis) phases. The cell cycle is regulated by various proteins that include Cyclins, Cyclin-dependent kinases (**CDK's**), and Cyclin-dependent kinase inhibitors (**CDKI's or KIP's**) (See Figure 1.2). The levels of Cyclins rise and fall with the various stages of the cell cycle (Kimball 2003). On the other hand, levels for CDK's remain stable (Shah 2001). They can only be activated by binding to the appropriate Cyclin (See Figure 1.3). The CDK/Cyclin complexes add phosphate groups to protein substrates, which in turn,

control processes in the cell cycles (Kimball 2003). As a cell progresses through the cell cycle, it is promoted by CDK's, which in turn are either positively or negatively controlled by Cyclins (substrates which determine which are phosphorylated). The Figure 1.2 below represents the relationship between Cyclins and CDK's. Also important are the CDK/Cyclin complexes. Figure 1.3 illustrates binding properties and structures of Cyclin/kinases. Changing a substrate to either promote or inhibit binding, alteration of residues and certain substrates could be a controlling factor in the cell cycle process to control proliferation.

Throughout the process of cell division, various checkpoints may halt the process and lead to cell cycle arrest. These factors include: DNA damage (G1 and G2 phase arrest), unreplicated DNA (S phase arrest), and improper spindle formation (M phase arrest). For examples, in order to exit G_0 growth signals must induce expression of response genes, which in turn, phosphorylate transcription factors. Next, in order to exit G_1, E2F transcription factors induce Cyclins A, E, and CDK2. Also, E2F's are inhibited by binding Rb. Cyclin D and CDK4/6 complexes phosphorylate Rb, which releases E2F's.

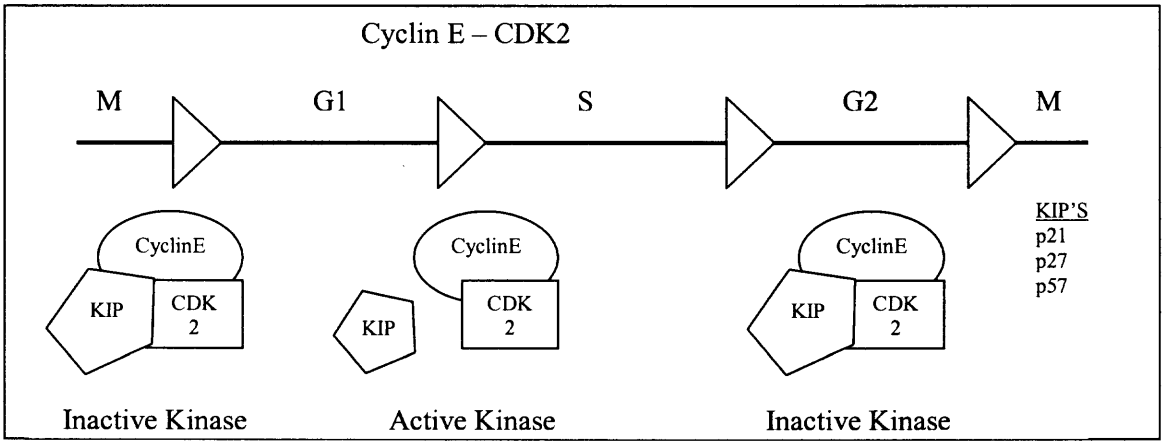

Figure 1.2 The Cyclin E/CDK2 complex: Activation based on KIP removal.

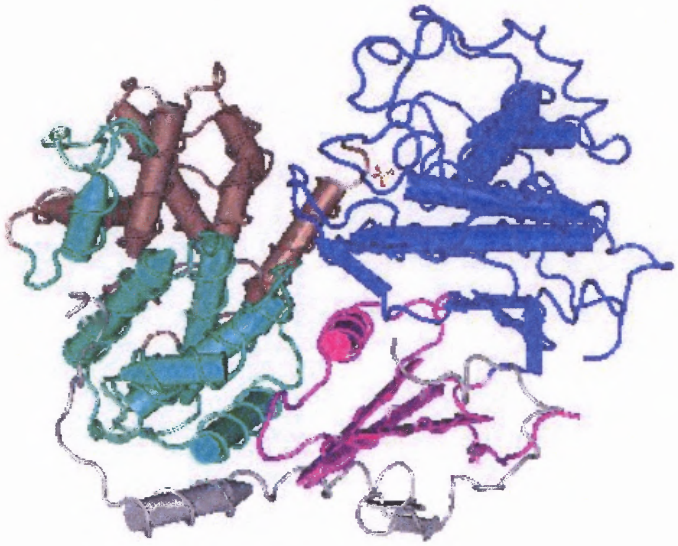

Figure 1.3 A p27(KIP1)Cyclin A/CDK2 complex: p27Kip1 binds the complex as an extended structure interacting with both Cyclin A and CDK2. On Cyclin A, it binds in a groove formed by conserved Cyclin box residues. On CDK2, it binds and rearranges the amino-terminal lobe and also inserts into the catalytic cleft, mimicking ATP. The five different colors represent domains (Russo 1996).

This cycle of cell division plays an important role in the response of cancer cells to therapy. Many anti-cancer therapies are designed with the intent to target a specific phase in the cell cycle (See Table 1.1). With synchronization, biopsy samples showed the cell cycle genes CDK4, Cyclin D3, and RING3 had a clear pattern of circadian expression (Grundschoeber 2003). Also, it is known that passage through G1 into the S phase is regulated by Cyclins D, E, and A. Cyclin B1 is involved in regulating the transition from G2 to the M Stage (Bjarnason 1999).

Table 1.1 Cancer Therapeutics and Points of Cell Cycle Interaction

G1 Phase	Steroid Hormones (i.e. Tamoxifen, Toremifene)
S Phase	Antimetabolites (i.e.Cytarabine, Mercaptopurine, Methotrexate, 5-Flourouacil)
S/G2 Phase	Etoposide
G2 Phase	Bleomycin
M Phase	Vinca Alkaloids (e.g., Vincristine, Paclitaxel)

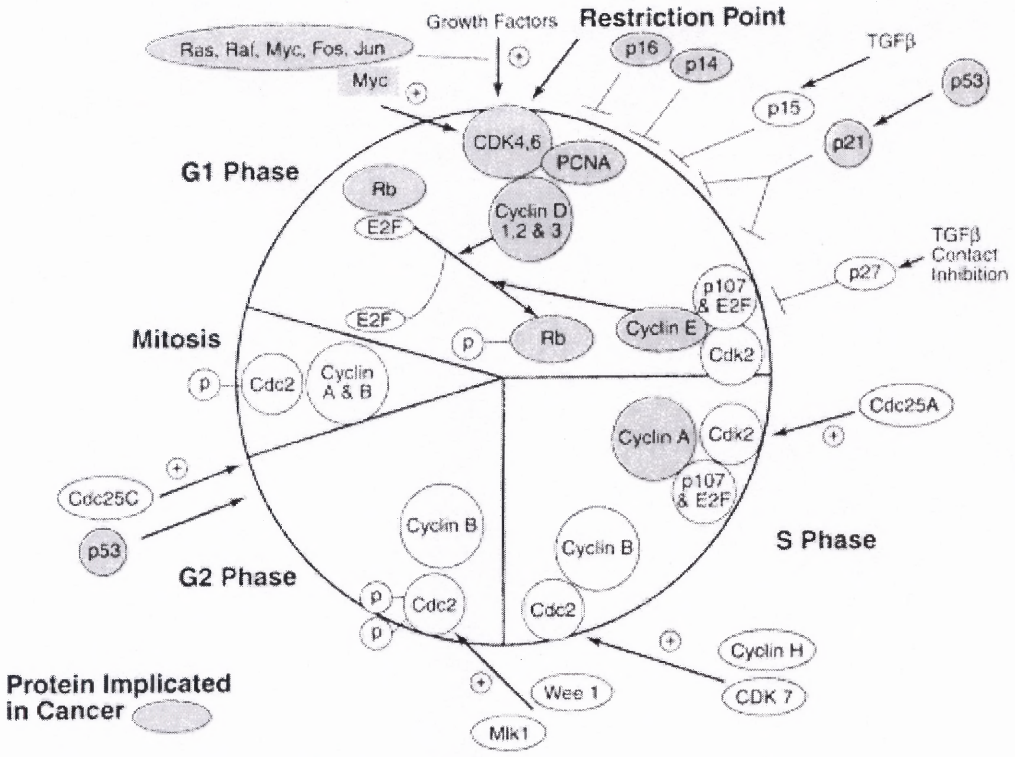

Figure 1.4 Various cell cycle protein interactions (Sielecki et al., 2000).

As shown in Figure 1.4, there are many interactions involved in the cell cycle and checkpoints that control the progression to the next phase. If these checkpoints are not met, progression halts and proliferation does not ensue. Interactions of these proteins and their inhibitors were studied. The proteins that were tested in this study include the expression of Cyclin/CDK complexes at various cell cycle stages. In the G1 stage, the Cyclin D1/CDK2, CDK4 complexes; in stage Late G1, the Cyclin E/CDK2 complex; in stage S, the Cyclin A/CDK2, complex; and in stage G2, Cyclin A, B1/CDK1 complex. Also studied were the KIP's 21, 27, and 57, as well as the apoptosis proteins c-JUN and PJNK, and the proliferation marker PCNA.

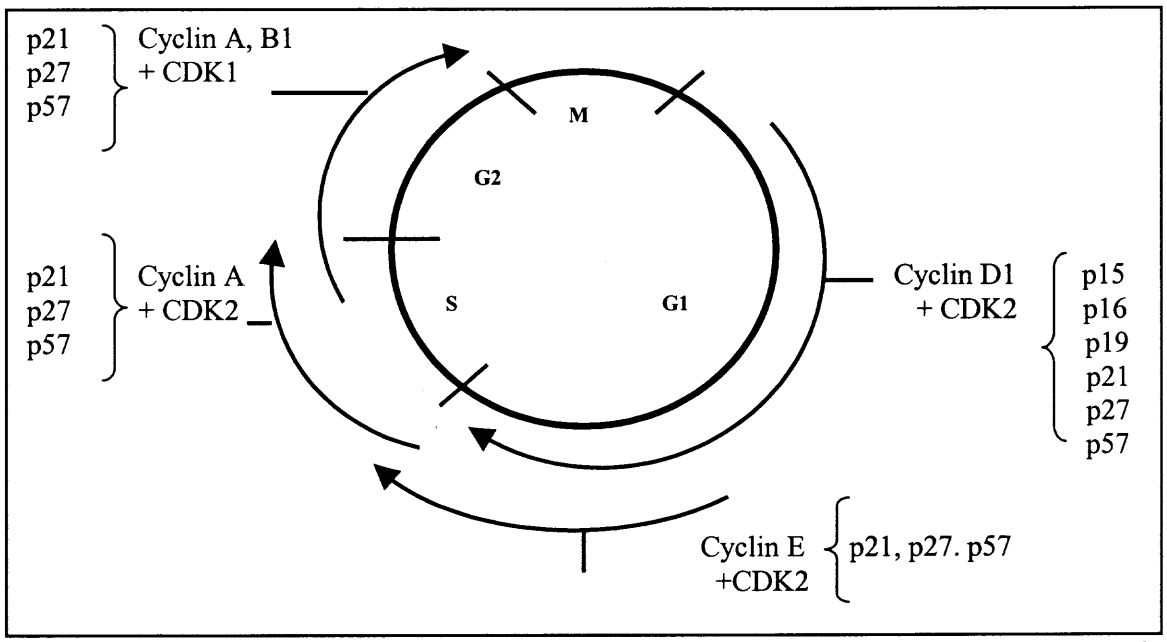

Figure 1.5 Expression patterns of cell cycle and apoptosis proteins. The cell cycle is forward regulated by growth factors (i.e. VEGF), oncogenes (i.e. Myc), Cyclins (i.e. A,B1,D1,E), and CDK's (i.e. 2,4,6). It is blocked by tumor suppressor genes (i.e. Rb, p53) and CKD inhibitors (i.e. p21, p27, p57).

Apoptosis also plays a role in prostate cancer. Apoptosis is a normal series of events in a cell that lead to its death (and then replacement). Studies have shown that apoptosis occurs via two distinct cellular pathways. The "extrinsic" pathway is activated by the absence of growth factors, hormones, or binding of death activator proteins to the cell surface. The "intrinsic" pathway is activated by intracellular signals, such as damage caused by radiation or cytotoxic factors. Both pathways converge inside the cell, and activate a family of proteins known as caspases. Caspases function by cutting proteins inside the cell and become activated early in apoptosis. Once a caspase is activated, the cell death process is irreversible. Finding the trigger to activate the caspase would lead to controlling cell death and survival (NCI 2003).

Cancer cells normally avoid apoptosis (Harnessing Apoptosis to Destroy Cancer Cells 2003). The goal of many cancer therapies is to induce apoptosis of the malignant cells. Binding of death-activator proteins (i.e. TNF-alpha, TNF-beta, and FasL) to the cell surface can trigger apoptosis. A protein of interest being studies is TRAIL from the TNF family, particularly for its greater effect on cancer cells when compared with normal cells (Weissman 2003). Factors such as cellular adaptations and mutations can prevent apoptosis and create a resistance to therapies.

Apoptosis and cancer were first linked in 1988 (NCI 2003). Patients with follicular lymphoma were found to have an overactive bcl-2 gene in B cells (an immune cell). The bcl-2 gene is normally considered a "brake" gene, in that it produces a protein that blocks apoptosis. When the gene was over actively expressed, anti-apoptosis proteins were produced in abundance resulting in cancer cell growth. This led to the finding that increased cell division could be attributed to cancer, however, cells could also promote tumor growth by avoiding programmed cell death (NCI 2003). The protein bcl-2 found on the mitochondria prevents apoptosis by blocking the release of cytochrome c from inside the mitochondria resulting in resistance to many therapies such as cisplatin and paclitaxel (Shah 2001). Often, Bcl-2 is present in abundance in cancers such as colon, lymphoma and leukemia. By decreasing expression of Bcl-2 levels or increasing expression levels of the pro-apoptotic protein BAX, and a natural inhibitor of Bcl-2, sensitivity to therapy can be restored (Weissman 2003).

Another critical protein in regulating the cell cycle and apoptosis is the tumor suppressor protein p53. The p53 protein is the gene most frequently disrupted in cancer. The p53 protein acts as a tumor suppressor because it either blocks the cell division of a

genetically damaged cell or triggers apoptosis by causing damage to the mitochondria and cytochrome c release. In 55 to 70 percent of human cancers, however, genetic mutations render the p53 protein deficient and cells with DNA damage can continue to accumulate. Loss of p53 function is associated with tumor aggressiveness and resistance to anti-cancer treatments (NCI 2003). Protein p53 serves as a checkpoint. At the time of DNA damage or oncogene stimulation, the p53 sends a signal to halt the cell cycle to prevent the cell from becoming cancerous. It is a DNA-binding protein involved in regulating the expression of genes involved in cell cycle arrest. Both CDK1 and CDK2 are thought to keep p53 in the cytoplasm when the cell is not in G1. Activity of CDK2 (by binding to Cyclin E or Cyclin A) is increased at the end of G1, which then phosphorylates p53 and removes it from the nucleus so it does not interfere with DNA synthesis. One such example includes tumor cells with a mutation in the p53 gene, which has proven to show a resistance to apoptosis under chemotherapy. One of the functions of p53 is to stimulate the expression of $p21^{CIP}$, which stops the transition from G1 to G2 until damage to the DNA is repaired. The mutant p53 allows the DNA damaged cells to replicate.

Apoptosis proteins used in this study include: p21, p27, p57, PCNA, and c-JUN. The protein p27 binds to Cyclin and CDK blocking entry into S phase (Ka et al., 1998). All of the interactions between cell cycle and apoptosis have a controlled and patterned rhythm. It is this rhythm which, when studied can lead to variations in cell proliferation and apoptosis.

1.4 Circadian Rhythms

Circadian rhythms are repeating cycles with a period length of about 24-hours. In a biological system, this means that there exists: a rhythmic fluctuation in gene expression patterns, a rhythm that is endogenous, and a rhythm that can be reset by external stimuli. These endogenous rhythms oversee our daily events such as sleep, activity, hormone secretion, cellular proliferation, and metabolism (Healthlink 1999). Studies have shown that between 2-10% of all mammalian genes are clock-controlled genes (Richardson 2003).

These circadian rhythms in the body are coordinated by the suprachiasmatic nucleus (SCN), a biologic clock located at the bottom of the hypothalamus (Healthlink 1999). The main circadian rhythm is known as the rest-activity cycle. The SCN is able to maintain an approximate 24-hour cycle of activity *in vitro/in vivo* and helps the organism adjust to environmental cycles. The SCN receives input from the retinohypothalamic tract (RHT), intergeniculate leaflet (IGL), raphe nuclei, the paraventricular thalamus and the limbic telencephalon. The projections from the retina are received by the SCN via the RHT, which comes from a subset of photoreceptors and retinal ganglion cells specialized for sensitivity to luminescence (Richardson 2003).

The IGL plays a role in photic entrainment and projects back to the SCN, terminating in areas that overlap the direct RHT-SCN projections. The IGL also plays an important role in non-photic entrainment stimuli such as motor activity. Electrical stimulation of the IGL produces phase shifts similar to those produced by activity (Richardson 2003). Signals from the SCN travel to several brain regions, including the pineal gland, which responds to light-induced signals by switching off production of the

hormone melatonin (Healthlink 1999). The raphe nucleus communicates with the SCN to show a direct suppressive effect of serotonin on SCN neuronal firing (Richardson 2003). The duration of SCN cycles are calibrated by the alternation of light and darkness.

Cellular metabolism and proliferation also display rhythms in normal tissues, which may be affected by the rest-activity cycle (See Figure 1.6). Because of the SCN's control over metabolism and proliferation, further studies may allow us to observe central and peripheral coordination of clock function and cancer growth, new vessel function, and capillary permeability. A study with cultured fibroblasts showed a mechanism similar to a circadian clock after synchronization with a serum shock treatment. With monitoring every four hours for a total of 76 hours, this proved to be a simple model to research circadian gene expression (Grundschober et al., Duffield et al., 2002). If one could learn how to use predictable changes in cellular metabolism or proliferation along the 24-hour timescale, one might be able to improve treatments for diseases such as cancer.

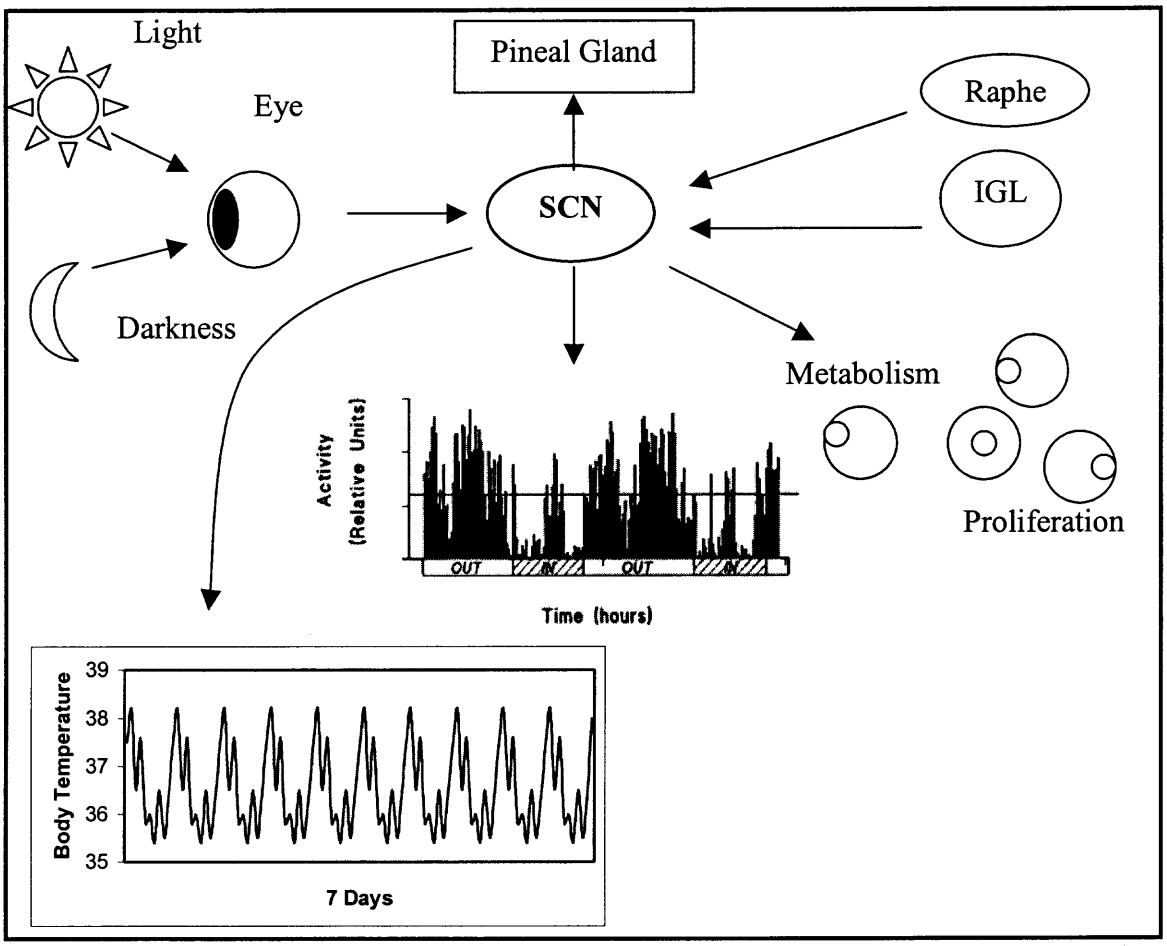

Figure 1.6 Schematic view of the circadian system. The SCN is the central pacemaker located in the hypothalamus. It is entrained to the dark/light cycle by stimula from the retina. The SCN effects metabolism, proliferation, the rest activity cycle as well as circadian body temperature (Mormont 1997).

1.5 Chronotherapy

Chronobiology is the branch of biology concerned with the periodicity occurring in living organisms (Kobayashi et al., 2002). From learning about periodicities of various cell cycle and apoptosis proteins, chronotherapy can be understood and developed. Chronotherapy is a type of therapy used by administering a treatment as a function of rhythms. Clinical trials have confirmed the overall ability to deliver higher doses of chemotherapy and the improvement in clinical outcome by incorporating these

chronobiological principles. Studies in different areas have been proven with these principles. For example, a study was carried out measuring peak tumor uptake between normal tissue and chemotherapeutics as a function of the time of day doses were given. The dosing with chemotherapeutics had a peak tumor uptake at 11:00 PM and peak hour of normal tissue dosing was at 5:00 PM. This was thought to be because of the unique periodicity of tumor blood flow compared with the rhythm of normal tissue blood flow, and both being dependant on the time of day (Blumenthal et al., 2001).

Tumor treatments with cytokine IL-12 were studied and found to be governed by biological rhythms, which may be regulated by rhythmic change in the expression of IL-12 receptor and interferon-gamma receptor (Alisauskas et al., 1999). Another tumor treatment, the newly developed COX-2 inhibitory drug celecoxib has also been found to incorporate principles of chronotherapy and chronotoxicity. (Blumenthal et al., 2002). Studies are also being carried out evaluating chronotherapy using three dietary agents, which are vitamin D_3, curcumin, and Selenium (Blumenthal et al., 2002). These experiments are aimed at detecting rhythmic changes in tumor response, host tolerance, and drug pharmacology, evaluated with several chemotherapeutic agents in order to determine the optimal time of day to dose a patient with a particular therapeutic agent (Blumenthal et al., 2002). In addition, studies have shown that optimally timed cancer chemotherapy with doxorubicin or pirarubicin (06:00h) and cisplatin (18:00h) enhanced the control of advanced ovarian cancer while minimizing side effects (Kobayashi et al., 2002).

1.6 Selenium as a Therapeutic Agent

Selenium is an essential trace mineral found in the human body (National Research Council, 1989). Selenium (Se) is a part of the enzyme glutathione peroxidase, which metabolizes hydroperoxides (Combs et al., 1997). Generally, selenium functions as an antioxidant that works in conjunction with Vitamin E. Plasma levels vary from 8 to 25 μg/dL (1.0 to 3.2 μmol/L), depending on selenium intake (Combs et al., 1998). Part of selenium function is to protect cells against the effects of free radicals that are produced during normal oxygen metabolism. The body has developed defenses such as antioxidants to control levels of free radicals because they can damage cells and contribute to the development of some chronic diseases (Combs et al., 1998). Selenium is also needed for normal functioning of the immune system and thyroid gland, which is important in various diseases including cancer. Some studies indicate that mortality from cancer, including lung, colorectal, and prostate cancers, is lower among people with higher selenium blood levels or selenium intake (Russo et al., 1997). The criteria for chemopreventive agents are experimental and rely on epidemiological data showing efficacy, safety on chronic administration, and a mechanistic rationale for activity (Clark 1998). At this time, selenium is seen more as a chemopreventative agent. However, studies are in progress to prove that selenium may be used as a therapeutic agent against prostate cancer. Selenium has been shown to influence the risk of cancer. PC-3 prostate tumors in particular have been shown to be affected and their growth slowed (Combs et al. 1998). Some studies on the effects of selenium on prostate cancer are described below. Studies with a 200 mcg supplementation of selenium daily, did not affect recurrence of skin cancer, but significantly reduced total mortality and mortality from additional

cancers studied. The incidence of prostate cancer, colorectal cancer, and lung cancer was lower in the group given the selenium supplements (Combs et al., 1997).

Dong et al., carried out experiments to test the cellular and molecular effects of methylseleninic acid (MSA) against the human prostate carcinoma PC-3, *in vitro* (Dong et al., 2003). Cells exposed to various concentrations of MSA, showed dose-dependant and time-dependant growth inhibition. Cell cycle progression was slowed at multiple time points without effect to cells in different phases. Results were analyzed using flow cytometry, and annexin V- and propidium iodide-labeled cells demonstrated apoptosis induction by MSA. The human genome chip U95A from Affymetrix was also used for array analysis and then applied to profile the changes due to gene expression that might change the effects of selenium. A timed array was set up to establish gene expression at 12, 24, 36, and 48 hours after selenium treatment. This identified a large number of genes that had various biological functions, yet all were classified to be responsive to selenium. Gene expression of 10 genes involved in cell cycle regulation was selected, and Western Analysis was performed to support the information from the array data. There seemed to be a 70% consensus between the two experiments. Dong concluded that genes such as GADD153, CHK2, $p21^{WAF1}$, Cyclin A, CDK1, and DHFR might change cell cycle progression because of the interaction with MSA The information may also provide insight to the effect of MSA on DNA repair, cell invasion, stimulation of growth factors, and the overall biological effects of selenium. The work in my thesis will expand on these studies to determine how selenium treatment at various times during a 24-hour day affects expression of various cell cycle and apoptotic proteins.

In another study, researchers compared the toenail selenium levels of nurses with and without cancer. They did not find any apparent benefit of higher selenium levels (Garland et al., 1995). These conflicting results emphasize the need for additional research on the relationship between selenium and chronic diseases such as cancer. A study that may help answer some of the questions about the effect of selenium supplementation on cancer risk has started in France. The Supplementation en Vitamines et Mineraux Antioxydants, or SU.VI.MAX Study, is a prevention trial that is providing doses of antioxidant vitamins and minerals that are one to three times higher than recommended intakes, including a daily supplement of 100 mcg selenium. More than 12,000 men and women are being followed for eight years to determine the effect of supplementation on the incidence of chronic disease, such as cancers and cardiovascular disease (Hercberg et al., 1998).

Yet further studies found selenium in the form of selenized brewer's yeast (200 g Se/day) was associated with a 63% reduction in prostate cancer in a cohort with prior nonmelanoma skin cancer compared to placebo-treated controls (Clark et al., 1998). Selenium has been studied as a preventative medicine in all forms in more than one form of cancer. This study focuses on the chronotherapy of selenium on human prostate xenografts.

CHAPTER 2

MATERIALS AND METHODS

2.1 Cell Culture

Prostate cancer cell lines ALVA-31 and PC-3 were grown in Complete Dullbecco's Modified Eagle's media, (DME, Irving Scientific, Santa Ana, CA). The solution was made up of 10% (50 ml/500 ml) Fetal Bovine Serum (FBS, Ityclone, Logan, UT), and 1% (5 ml/500 ml) other additives including Nonessential amino acids, L-glutamine, Penicillin/Streptomycin, and Sodium pyruvate. The cell lines grew confluent in between 1-2 weeks when the cultures were incubated (Forma Scientific, HEPA filter) at 37° C. Trypsin (Irving Scientific, Santa Ana, CA) diluted to 1X (3 ml) was used to harvest cell lines. Equal volumes of media were added and centrifuged at 1400 rpm for 5-minutes. When confluent, 8 µl of trypan blue dye (SIGMA Chemical Co., St. Louis, MO) and 8 µl of the suspension of ALVA-31 cells were placed into a culture tube. The solution was mixed by pipette and 10 µl were counted using a hemacytometer (Bright-Line, Horsham, PA). The cells were counted under a microscope (Olympus CK2, Newark, NJ) at a 6x setting. Four by four blocks were added, averaged and then multiplied by 20,000 to set cells/ml. Mice were injected with 1×10^7 cells/mouse.

To create a single suspension, the cells were passed through syringes of sizes 23-, 25-, and 27-gauge. Cell suspensions used for the injections were set up using equal volumes (~5 ml) of cells suspended in media, and Matrigel Basement Membrane (BD Biosciences, San Jose, CA).

2.2 Chronotherapy Models

Severe Combined Immunodeficiency (SCID) mice were used in this study. These mice lacked both T & B cells due to a defect in recombination, and therefore, easily accepted foreign transplants. In general, they are very useful models for testing various immunity and disease responses. They also demonstrate *in vivo* growth patterns of normal and malignant tissue. Twenty-eight SCID mice per tumor line were placed into rooms with defined 12 hour on and 12 hour off periods of light (see Table 2.1) two weeks prior to subcutaneous implantation of 200 ul of PC-3 and ALVA-31 cell suspension. The tumors were allowed to grow in their respective HALO for approximately two weeks to a size of .500 g. A total of 56 mice were treated with sodium selenite (28 for each prostate carcinoma line). The mice were given a dose of 30 micrograms of sodium selenite (98% purity) (Sigma Chemical) per mouse per day for four days. Intraperitoneal injections (i.p.) were administered at one of seven HALO. Times of injection are shown in the Table 2.1. Animal weight, tumor size, and temperature in the HALO rooms were monitored. If there were any signs of lethargy, weight loss (<14.0 g), or death, the mice were removed from their respective HALO.

Table 2.1 Cycles of Light/Dark Patterns for Three Mouse Rooms Used in Studies

	AM									PM											AM				
Time	7	8	9	10	11	12	1	2	3	4	5	6	7	8	9	10	11	12	1	2	3	4			
Injection		▼	▼	▼	▼	▼		▼	▼																
Room 1													■	■	■	■	■	■	■	■	■	■			
HALO	24	1	2	3	4	5	6	7	8	9	10	11	12	13	14	15	16	17	18	19	20	21			
Room 2	■	■	■	■	■	■	■	■	■																
HALO	15	16	17	18	19	20	21	22	23	24	1	2	3	4	5	6	7	8	9	10	11	12			
Room 3				■	■	■	■	■	■	■	■	■	■	■	■	■	■	■							
HALO	9	10	11	12	13	14	15	16	17	18	19	20	21	22	23	24	1	2	3	4	5	6			

Placing the mice two weeks prior was to ensure the synchronization of the biologic rhythms to a new light/dark regimen. The **H**ours **A**fter **L**ight **O**nset (HALO) was determined by the hour the light went on in the room. The HALOs were selected so that various time point studies could be carried out in span of a normal workday (See Table 2.2). The temperature in each room was approximately uniform at about 22+/- 2° C. Four mice per tumor per treatment (tumors ALVA-3 and PC-3 treated with sodium selenite, tumors ALVA-31 and PC-3 untreated) were placed in each HALO to be studied. Black triangles (See Table 2.1) show the times of the injections. The gray area depicts the times and the rooms for injections, while the black shaded boxes represent times in each room where the HALO cycle signified darkness (night).

Table 2.2 HALO Time Conversion

HALO	3	7	10	13	17	20	23
TIME	10:00AM	1:00PM	4:00PM	7:00PM	11:00PM	2:00AM	5:00AM

2.3 Tissue Homogenization and Protein Content

After 2-5 weeks the SCID models were sacrificed and the organs (lung and kidney) were removed from the untreated models of ALVA-31. The organs were washed, blotted, weighed, and flash frozen with 100% alcohol. All tumors samples (treated and untreated) were also removed in the same manner. For homogenization, ½ ml of extraction buffer was prepared per 100 mg of tissue. The extraction buffer consisted of: 25 mM Tris (SIGMA Chemical Co., St. Louis, MO) at a pH of 7.4, 100 mM of NaCl (SIGMA Chemical Co., St. Louis, MO), and 20 mM of NH_4HCO_3. The extraction buffer was added to the samples in amounts based on the weight of the tumor and the sample/extract

was homogenized using a PRO300PC Programmable Laboratory Benchtop Homogenizer (Monroe, CT). The 2 ml samples were centrifuged at 10,000 rpm for 20 minutes at 4 °C (Eppendorf Centrifuge 5417R). The supernatants were then placed into 3 ml eppendorf's and stored in a –20 °C freezer.

Bradford Reagent (SIGMA Chemical Co., St. Louis, MO) was used to determine total protein concentration in solution. Two sets of test tubes were labeled, and a five-fold dilution was prepared with 100 µl of samples in the first set of test tubes. Next, 200 µl of extraction buffer was added and 5 µl of protease inhibitor Leupeptin(3) serine and cystein proteases, soluble in H_2O (1 mg/ml). For the standard curves, 100 mg/ml of Bovine Serum Albumen was used for the dilutions. The standard curve of net absorbance was determined by setting up an assay (See Table 2.3).

Table 2.3 Protein Standard Concentration Assay

Tube	Buffer Sample (ml)	[BSA] Protein Standard (mg/ml)	Bradford Reagent (ml)	Absorbance 595 (nm)
1	0.1	0	3	0.126
2	0.1	0.1	3	0.429
3	0.1	0.25	3	0.667
4	0.1	0.5	3	1.043
5	0.1	1.4	3	1.252
6	0.1	2.0	3	1.441

The Bovine Serum Albumen standards used were: 0, 0.25, 0.5, 0.75, and 1.0 mg/ml. Then, 3 ml of Bradford Reagent was added to the 100 µl of protein. The binding of the dye to protein caused the peak absorbance of the dye. Unbound Brilliant-Blue G dye absorbs light maximally at a wavelength of 465 nm, while the absorption maximum

is at 595 nm when the dye is bound to protein. The absorbance of light by the dye-protein complex at 595 nm is proportional to the amount of protein bound. The reagent formed a complex between the dye (Brilliant blue G) and the proteins. The samples were vortexed for 2 seconds for uniform mixing and allowed to incubate for 40 minutes at room temperature. The samples were then transferred to cuvets and results were read by Beckman (Memory Pac Module) at an absorbance of 595 nm (A_{595}). Absorbance was recorded and the concentration was determined by comparison to a standard curve. The protein-dye complex lost stability after 60 minutes; therefore, the absorbance of the samples must have been recorded within that allotted time limit. This was used as a direct correlation to the concentration of the sample. After obtaining the results, plotting the absorbance vs. protein concentration created a standard curve for protein content. In theory, the amount of absorption should be proportional to the protein present. To determine the amount of protein concentration in each sample, the formula below was applied to the data sets using the equation from the plotted standards.

$$((A_{595} - \text{y-INTERCEPT})/\text{SLOPE}) * 5 \qquad (2.1)$$

Each sample was then diluted with additional extraction buffer (total volume = 300 µl with a final concentration of 6 ug/3ul using the formula shown below. These sample dilutions would then be used for multiple sets of antibody immunoblotting without having to thaw the original samples. This figure was then subtracted from the total volume to yield the amount of extraction buffer needed for the solution. Next, 300 µl samples were made and used throughout the immunoblots.

((2 * TOTAL VOLUME)/PROTEIN CONCENTRATION) (2.2)

2.4 Immunoblots

Protein electro-blotting (Western blotting) is a technique, first used in the 1970's to identify protein antigens that bound to specific antibodies. Since then, a modified protein blotting procedure called dot-blotting or immunoblotting has been developed whereby the protein extraction is applied directly to the nitrocellulose membrane as a small spot. Immunoblotting is a widely used technique for detection and identification of proteins using antibodies. Because the time-consuming steps of gel electrophoresis are no longer an issue, dot blotting has the advantages of being simple and rapid. Moreover, dot blotting is reported to be approximately 10- to 1000-fold more sensitive than western blotting. The antibodies bind to the proteins and secondary antibodies, detect them.

For this work, both apoptosis and cell cycle regulatory proteins were studied. Expression studies of the cell cycle proteins included: Cyclin A, B1, D1, E as well as Cyclin-dependant kinases (CDK's) 1, 2, 4, and 6 and KIPs: p21, p27, and p57. Expression of the apoptosis proteins c-JUN and PJNK and the proliferation marker, PCNA were also assessed.

Table 2.4 Cell Cycle and Apoptosis Antibodies Used in Immunoblots

Antibody Descriptions				
Primary Antibody	**Source**	**Type**	**Secondary Antibody**	**Specificity: Phase of Cycle**
Cyclin A	BD	Cell Cycle	Goat Anti-Mouse IgG1	G2, S
Cyclin B1	BD	Cell Cycle	Goat Anti-Mouse IgG1	G2
Cyclin D1	Oncogene	Cell Cycle	Goat Anti-Mouse IgG1	G1
Cyclin E	Oncogene	Cell Cycle	Goat Anti-Mouse IgG1	S, Late G1
CDK1	Oncogene	Cell Cycle	Goat Anti-Rabbit IgG1	G2
CDK2	Oncogene	Cell Cycle	Goat Anti-Rabbit IgG1	S, Late G1
CDK4	BD	Cell Cycle	Goat Anti-Mouse IgG1	G1
CDK6	Oncogene	Cell Cycle	Goat Anti-Mouse IgG1	G1
cdc25a	Santa Cruz	Cell Cycle	Goat Anti-Rabbit IgG1	G1
dp-1	Santa Cruz	Cell Cycle	Goat Anti-Mouse IgG1	S
p21	BD	Apoptosis	Goat Anti-Mouse IgG1	All
p27	Oncogene	Apoptosis	Goat Anti-Mouse IgG1	All
p57	Oncogene	Apoptosis	Goat Anti-Mouse IgG1	All
c-JUN	Santa Cruz	Apoptosis	Goat Anti-Rabbit IgG1	All
PCNA	BD	Apoptosis	Goat Anti-Rabbit IgG1	All

A nitrocellulose membrane (Optitran, Scheicher & Schuell, Keene, NH) with a pore size of 0.45 µl was used to create a 7 x 4 grid (See Figure 2.1) of the protein samples in accordance to the number of samples used. Approximately 3 µl of each of the protein samples were placed on the membrane and allowed to dry for 30-minutes in a humidified chamber.

Sample #	HALO 3	HALO 7	HALO 10	HALO 13	HALO 17	HALO 20	HALO 23
1	●	●	●	●	●	●	●
2	●	●	●	●	●	●	●
3	●	●	●	●	●	●	●
4	●	●	●	●	●	●	●

Figure 2.1 Example of Immunoblot grid.

The membrane was then placed in Trizma Buffered Saline (TBS). This was made in 2000 ml solution using 24.8 g Trizma Base (SIGMA Chemical Co., St. Louis, MO), 18.0 g Sodium Chloride (SIGMA Chemical Co., St. Louis, MO) 28.0 ml HCL (SIGMA Chemical Co., St. Louis, MO), and brought up to 2000 ml with distilled H_2O. The solution was then calibrated to a pH of 7.5 and used throughout the procedure.

Next, the membrane was placed in 100 ml of blocking solution, which consisted of 5% dry non-fat milk (Nestle Carnation Instant Dry Milk, Solon, OH) in TBS for a two hour shaking wash on a rotating table at a speed of 60 rpm. This rotation speed was constant throughout the procedure. The blocking solution was then poured off and the membrane was then incubated with a (1:2000) dilution of a primary antibody (See Table 2.4) for 1 hour on the rotating table. The antibody was rinsed with TBS, followed by two 5 minute shaking washes with TBS. The membrane was then incubated with a (1:2000) dilution of the corresponding biotinylated secondary antibody (Vector Labs, Burlingame, CA) for 30 minutes on the rotating table (See Table 2.4). The secondary antibody, made in goat, came in 1 mg/ml concentrations and diluted in PBS. During the incubation, an **A**vidin and **B**iotinylated horseradish-peroxidase macromolecular **C**omplex (ABC) reaction (Vectastain Peroxidase Standard PK-4000, Vector Laboratories, Burlingame, CA) was made and left to incubate for 30 minutes. This was used to create a horseradish peroxidase conjugate. At the end of the 30 minute secondary antibody incubation, the membrane was rinsed with TBS followed by three 5 minute shaking washes on the rotating table. The ABC reaction was then brought up to 50 ml with TBS and poured on the membrane for 30 minutes. Another set of three 5 minute washes with TBS followed the ABC incubation. In order to detect antigens conjugated to the horseradish-peroxidase

antibodies, Luminol (ECL Plus Western Blotting, Detection Reagents, Amersham Biosciences) was prepared with a 40:1/A:B ratio with a final volume of 0.1 ml/cm2. In a non-polystyrene 15 ml conical vial, 2.73 ml of Solution A was added and 68.3 µl of Solution B. The total volume of the solution was 2.8 ml and the luminol was pipetted directly onto the membrane for 6 minutes.

Afterwards, the membrane was drained of excess luminal and wrapped in plastic and exposed to a sheet of film (Kodak X-OMAT AR, Scientific Imaging, Rochester, NY) in the darkroom for 10 minutes, and the film developed. Three blots per antibody were tested for statistical analysis. The film was scanned into the computer using a basic PhotoEd program included in the Windows system, and saved as a picture (.jpg) image. The program Un-Scan-It was used to calculate pixel density and quantify results. From the drop-down menu, Digitize was selected and Image (gel) was chosen. Next, the saved file was opened and "Segment Analysis Positive" was selected. On the next menu ODC (log) was checked and the screen showed the digitized sample. Boxes were placed around each immunoblot sample in order from 1 – 28 down each column until all the samples were boxed. The "Digitize" button was selected and then the "Exit" button. From the File menu, the gel data was saved including: Column titles, Pixel Total, Background, Maximum Pixel, and Average Pixel. This data was copied into an Excel spreadsheet for further analysis. The data was plotted and graphed in excel by means, medians, and standard deviations. The ANOVA and COSINOR methods were applied to these data sets to find correlations between the groups of treated tumors, untreated tumors, and organ sets.

2.5 ANOVA and COSINOR

Statistical analysis of results was performed by a one-way ANOVA, a two-way factorial ANOVA or one-tailed Student's t test, as stated. Cosinor analysis was used to analyze general rhythmic parameters, i.e., Acrophase (the maximum of the cosine function fit to the experimental data), Mesor (the statistical estimate of the 24-h time series mean) and Amplitude (half the difference between maximal and minimal values of the derived cosine curve). Percent of rhythm defined the part of variation that could be explained by a cosine function. Statistical significance of the derived cosine curves was tested against the null hypothesis (i.e., amplitude = 0); p values lower than 0.05 were considered evidence for statistical significance.

The acronym ANOVA is the ANalysis Of VAriance between groups. ANOVA performs comparisons like the *t*-Test, but for an arbitrary number of factors. Each factor can have an arbitrary number of levels. In addition, each factor combination can have any number of replicates. ANOVA works on a single dependent variable, and the factors must be discrete. Generally, multiple *t*-tests are carried out, but are difficult to use because as the number of groups grows, the number of needed pair comparisons grows quickly, and the numbers lose significance. The likely range of variation is given by thestandard deviation of the estimated means by using the calculation of the formula below:

$$\sigma/N^{1/2} \qquad (2.3)$$

This is where σ is the standard deviation of the size of all the samples and N is the number of samples in a group. The comparison between the actual variation of the group averages and that expected from the above formula is expressed in terms of the F ratio:

$$F = \frac{\text{(found variation of the group averages)}}{\text{(expected variation of the group averages)}} \quad (2.4)$$

Thus, if the null hypothesis is correct, F should be near one, whereas F greater than one, would indicate a location effect. The P-value reports the significance level. The number of degrees of freedom (d.f.) for the numerator (found variation of group averages) is one less than the number of groups. The number of degrees of freedom for the denominator (expected variation) is the total number of leaves minus the total number of groups. The F ratio can be computed from the ratio of the mean sum of squared deviations of each group's mean from the overall mean and the mean sum of the squared deviations of each item from that item's group mean ANOVA puts all the data into one number (F) and gives one (P) for the null hypothesis.

The COSINOR method involves the least squares fit to the data of a model that consists of one or more cosine curves with one or more periods anticipated to find trends. Cosinor analysis estimates the parameter of a cyclic phase. The data does not have to be in equal intervals. The analysis does require that the data can reasonably be considered to take the form of a deterministic cycle with a known period. Cosinor analysis entails curve-fitting the 24 hour profile to a cosine function, with estimates of the Acrophase (time of maximal concentrations), Mesor (mean level about which the 24 hour rhythm oscillates), and Amplitude. The calculation of the Mesor provides a more accurate estimate of the overall mean value, when compared with the arithmetic mean (which may

contain bias when the data are non-equidistant). When data are equidistant, the Mesor provides a smaller standard error. Measurement of the Acrophase allows a stable measure of timing of the overall high values, rather than time of a single value-based maximum. Once the three factors (Mesor, Amplitude, and Acrophase) are determined for the 7 time points of the various cell cycle and apoptotic antibodies, clustering of the amplitude-acrophase pairs can be estimated by the population mean cosinor method. This can be applied to multiple series from an antibody as well as the entire group of cell cycle or apoptosis antibodies. For this experiment P = 24 hours.

$$C(t) = \text{Mesor} + A \cos \frac{2\pi (t - \text{Acrophase})}{P} \tag{2.5}$$

CHAPTER 3

RESULTS

3.1 Protein Concentration

The absorbance vs. protein content are plotted for ALVA-31, PC-3 individually as well as with the Selenium treatment And for the normal organs (See Figure 3.1). The objective was to have a linear correlation graph. All graphs showed a two-point intercession on the slope of the standard curve. Plots with the tumor line PC-3 showed the closest relationship to the standard. The results showed a correlation to then help determine the dilutions needed for immunoblotting. The correlation coefficient of the r^2 value (See Formula 3.1) yielded the measurements in Table 3.1. If the plots were not towards a linear pattern and under the value of 0.900, then the dilutions were re-calculated. The lowest value was found to be among the ALVA-31 treated samples with an r^2 value of .9331 but still remained an acceptable value for the studies.

Table 3.1 The r^2 Values Determined For Protein Content

Tissue Type	r2 value	Tissue Type	r2 value	Tissue Type	r2 value
Lung	0.9719	Alva-31 Untreated	0.9455	PC-3 Untreated	0.9921
Kidney	0.9656	Alva-31 Treated	0.9331	PC-3 Treated	0.9965

$$r^2 = \frac{SS_{xy}{}^2}{SS_{xx}\, SS_{yy}} \qquad (3.1)$$

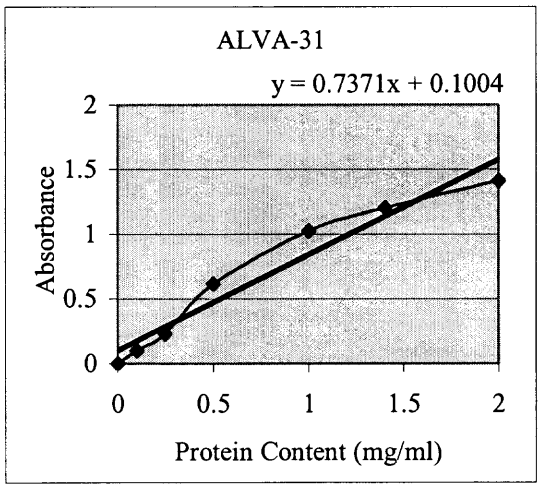

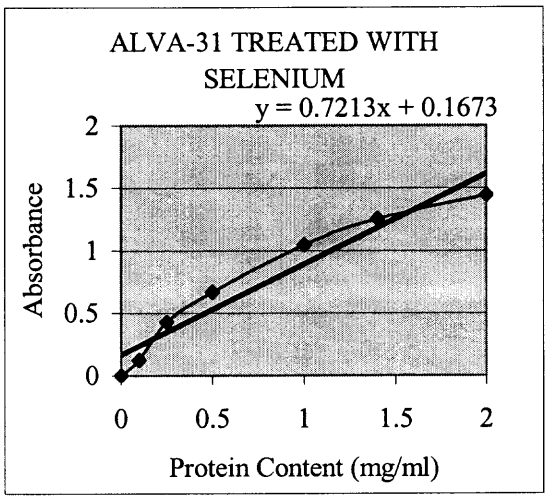

Figure 3.1 Standard curves for protein concentration vs. absorbance levels (1 of 3).

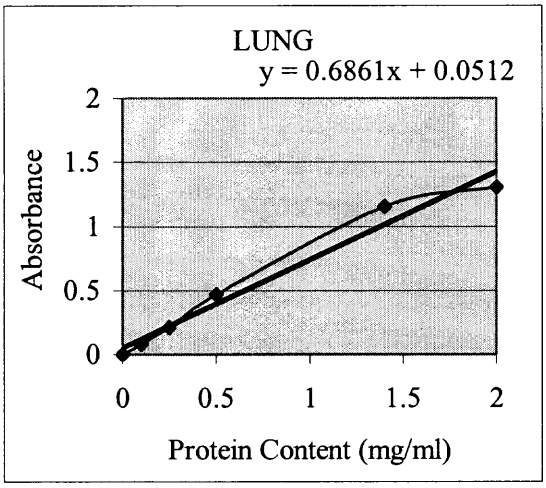

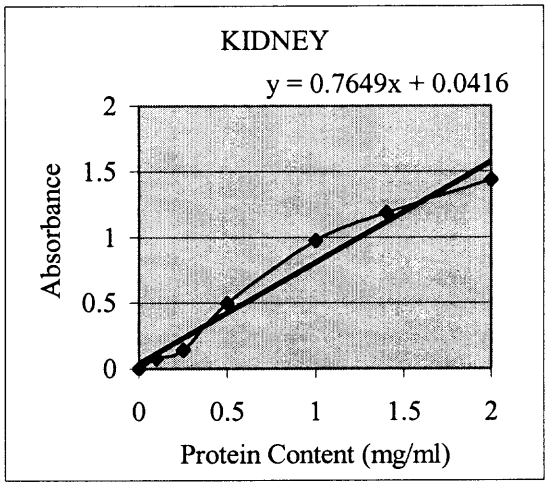

Figure 3.1 Standard curves for protein concentration vs. absorbance levels (2 of 3).

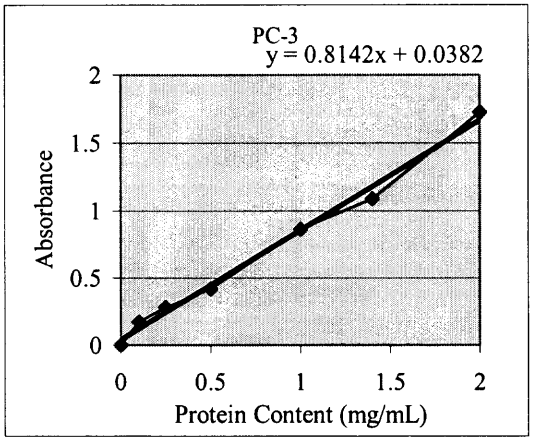

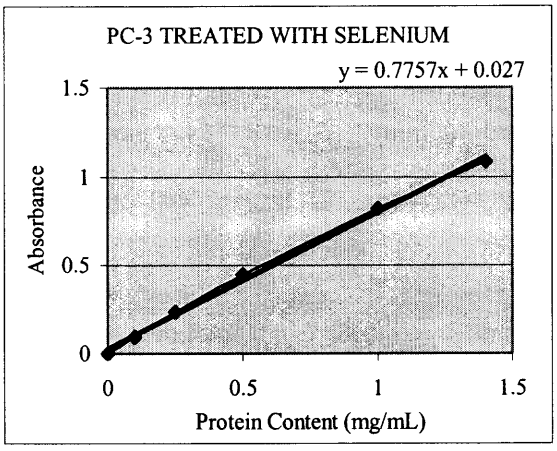

Figure 3.1 Standard curves for protein concentration vs. absorbance levels (3 of 3).

3.2 Immunoblot Data

Following the protocol for immunoblotting, the results varied greatly. Initially, results for PC-3 blotting showed that the chemiluminescent bound to the surfaces exposed around the protein blots but not to the blots themselves (See Figure 3.2). Also found was an unusual amount of background (See Figure 3.3). In order to address these (and following) issues, variables were changed until there were measurable results for analysis.

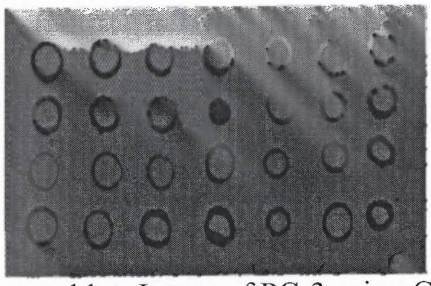

Figure 3.2 Immunoblot: Image of PC-3 using CDK2 antibody.

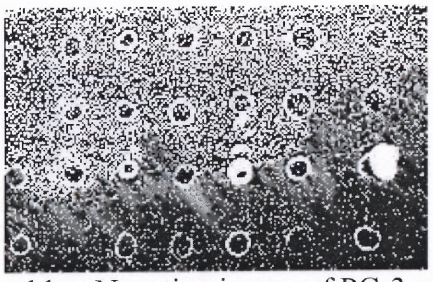

Figure 3.3 Immunoblot: Negative image of PC-3 using p57 antibody.

For the PC-3 blot shown in Figure 3.2, there was an issue with non-specific binding. Primary antibodies were checked to make sure that the correlating secondary biotinylated antibodies were being used. Some blots showed results like that seen in Figure 3.3. This problem was addressed by first trying to use a TBS solution from another laboratory, then by increasing the amount and timing of the TBS rinses. Also, the pH of the TBS was constantly checked to ensure a calibration of 7.4. Film exposure time

was increased from 10 minutes to an overnight exposure (16-18 hours). Increasing the amount of TBS, solved the problem of high background.

The ALVA-31 tumor blots treated with selenium yielded results, which showed very faint pixel density, if any (See Figure 3.4). The proteins CDK2 and CDK4 immunoblots were repeated, however still showed especially faint results with pixel densities scanned in between 0 – 8. These results were not included in this study but suggest that expression of these two CDKs was dramatically decreased to a level that could not be quantified.

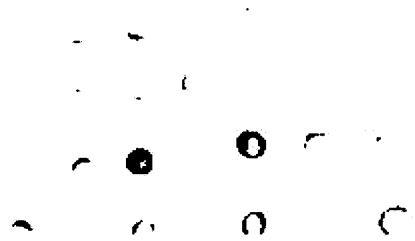

Figure 3.4 Immunoblot: ALVA-31 treated with selenium using Cyclin E antibody.

For these blots, additional primary and secondary antibodies (~25 µl) were added to the incubations. Also the lumigen used, SuperSignal West Pico Chemiluminescent Substrate (Pierce, Rockford, IL) was discarded and new lumigen was purchased. The ECL plus Western Blotting Detection System (Amersham Biosciences, Buckinghamshire, England) was used as a replacement lumigen. Fresh blocking solution was also created every morning to ensure that there was no contamination when left overnight. New nitrocellulose membrane was also ordered. Blotting was attempted with Dp-1, an additional cell cycle antibody, but the results remained the same. A test was run

using the DAB process with the c-JUN antibody, which yielded promising results and indicated that there was no problem with the original selenium treated samples.

For immunoblotting with both lung and kidney organ samples, a problem found was that the blots were over expressed (See Figure 3.5).

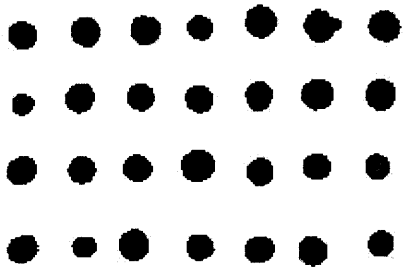

Figure 3.5 Immunoblot: ALVA-31 Liver.

To remedy this, the exposure time of the film was tested at 30 seconds, 1 minute, and 5 minutes. The optimal time of exposure for organ blotting resulted somewhere between 15-30 seconds to obtain some type of blot variation. Also, the amounts of primary and secondary antibody were reduced to 12.5 µl. By repeating the Immunoblot process and by changing variables as described standard blots were obtained for pixel density analysis (See Figure 3.6).

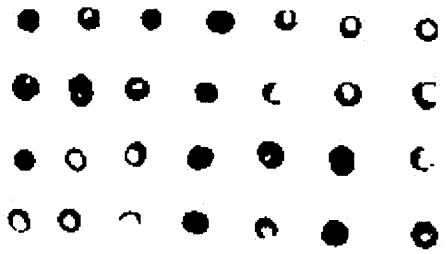

Figure 3.6 Immunoblot: ALVA-31 using p21 antibody.

Patterns of Cyclin and CDK expression for the cell cycle immunoblots varied with the progression of cells through the cell cycle. The expression for the apoptosis antibodies also showed variation. Organs expressed 255 pixel densities when left to expose over 1 minute, however showed variation at 15 seconds.

3.3 Organs: Lung and Kidney Analysis

Expression patterns for the lung and kidney were more stable than both the ALVA-31 and the PC-3 lines. There were high expression levels at every HALO for the organs. Although the cyclic expression rhythm found in the organs was not as great as the tumors, there were differences (low/high) points, which were studied. This pattern continued through cell cycle proteins for the lung, while the kidney results for cell cycle were more dispersed. The kidney tissues expressed CDK1 and Cyclin A with similar expression patterns. These two proteins interact during the G2 phase of the cell cycle. The ANOVA analysis was performed on normal tissue sets and the mesor, amplitude, mean, and acrophase were determined. These results were showed in Table 3.2 and Table 3.3. The values were segregated according to the phase of the cell cycle (G1, Late G1, S, and G2/M), or within Apoptosis or KIP categories.

In general, expression levels of antibodies used on kidney were more closely related in terms of acrophase as well as overall cyclic patterns. Although expression patterns of lung did not have many similarities, the overall range of pixel density was very close.

Table 3.2 Normal Tissue: Lung Expression Points

LUNG		
Apoptosis	Low	High
PCNA	23	20
c-JUN	20	7
KIP	Low	High
P21	3	23
P27	20	10
P57	20	17
Cell Cycle	Low	High
G1 Phase		
Cyclin D1	13	20
CDK2	20	7
CDK4	3	13
Late G1 Phase		
Cyclin E	7	10
CDK2	20	7
S Phase		
Cyclin A	17	20
CDK2	20	7
G2/M Phase		
Cyclin A	17	20
Cyclin B1	20	13
CDK1	20	7

Table 3.3 Normal Tissue: Kidney Expression Points

KIDNEY		
Apoptosis	Low	High
PCNA	N/A	N/A
c-JUN	7	20
KIP	Low	High
p21	20	10
p27	20	13
p57	20	3
Cell Cycle	Low	High
G1 Phase		
Cyclin D1	10	20
CDK2	7	10
CDK4	7	23
Late G1 Phase		
Cyclin E	23	13
CDK2	7	10
S Phase		
Cyclin A	3	20
CDK2	7	10
G2/M Phase		
Cyclin A	3	20
Cyclin B1	10	17
CDK1	3	20

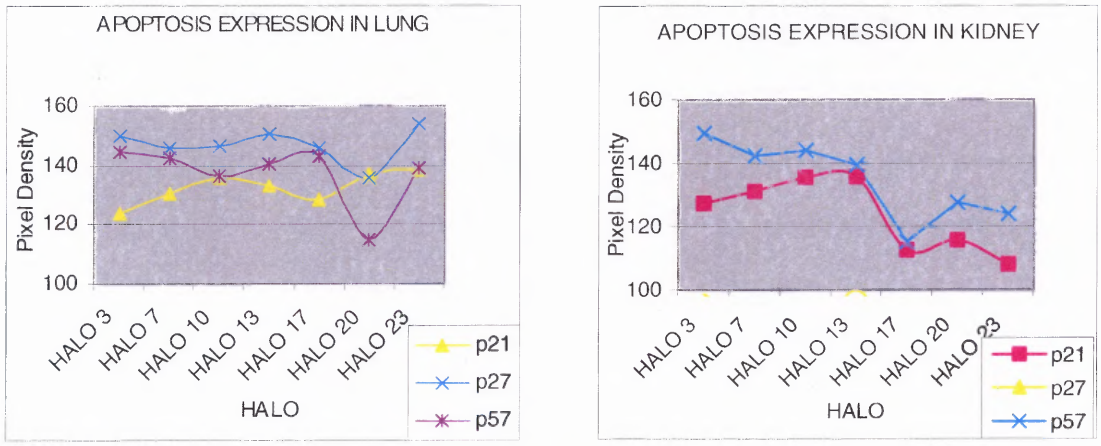

Figure 3.7 Organs Mean Graph of Apoptosis Proteins.

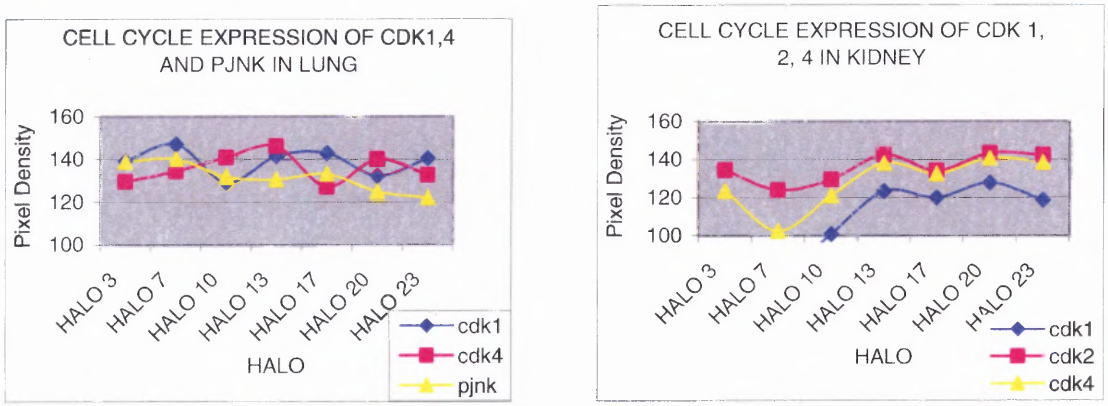

Figure 3.8 Organs Mean Graph of CDK's.

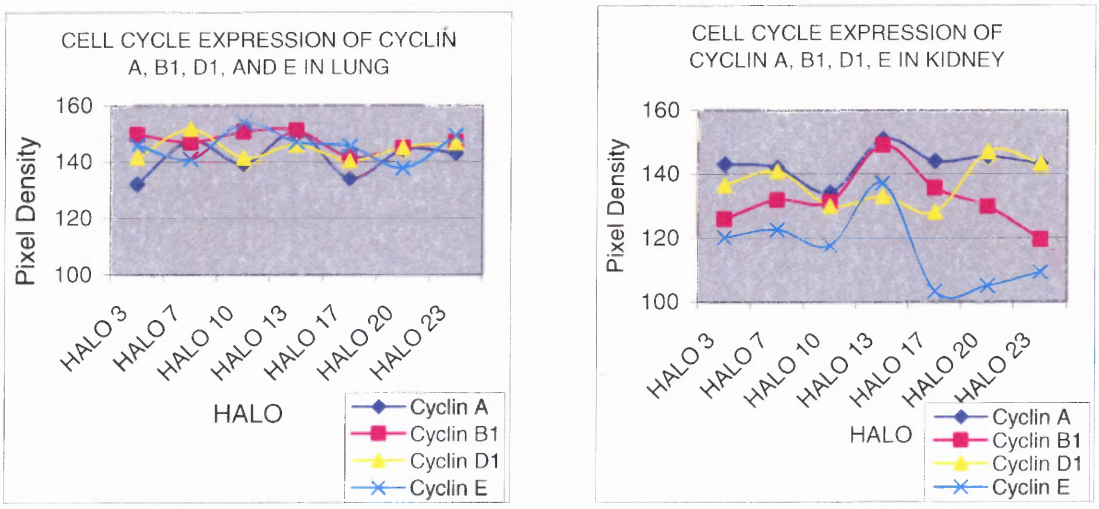

Figure 3.9 Organs Mean Graph of Cyclin's.

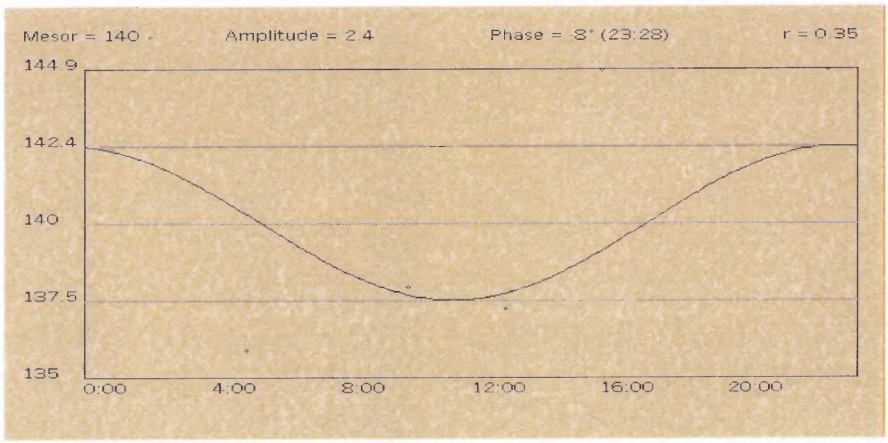

Figure 3.10 Kidney COSINOR using PCNA.

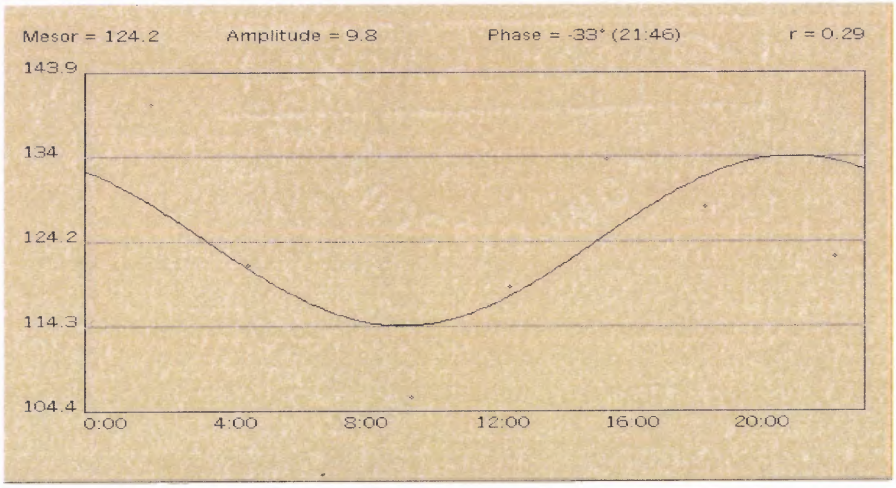

Figure 3.11 Lung COSINOR using CDK1.

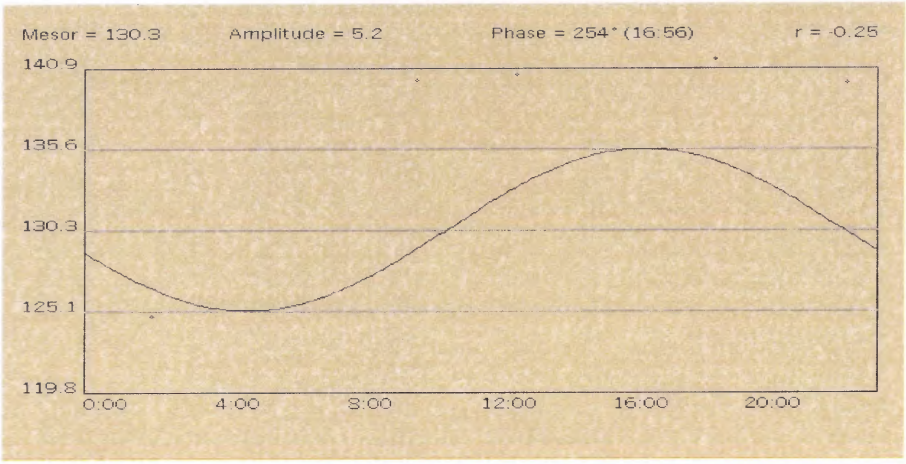

Figure 3.12 Kidney COSINOR using Cyclin E.

3.4 ALVA-31 Analysis

The means, standard deviations and medians were calculated from the scanned pixel data of the tumors and normal tissue. Bar graphs representing the medians of each HALO at various pixel densities were plotted (See Figures 3.15-3.18). The blue bars representing the untreated tumor, the red bars representing the tumors treated with sodium selenite, and the yellow bars representing the immunoblot data for the kidney. The same data values (acrophase, mesor, mean and amplitude) were also calculated for untreated and treated samples of ALVA-31 (See Tables 3.4 and 3.5).

For the HALO expression points of untreated ALVA-31, there was a clear pattern, in particular with the apoptosis and KIP's proteins, which showed a low expression at HALO 23 (5:00 AM). In general, for all cell cycle untreated ALVA-31 tumors, HALO 17 (1:00 PM) showed a low point of expression while HALO 13 (7:00 PM) showed a consistent pattern of high expression. The Cyclin A/CDK1 complex that forms in phase G2 had a consistent expression in ALVA-31 untreated samples across all HALOs. Both had a low expression point of HALO 17 (1:00 PM) and a high expression point of HALO 13 (7:00 PM). The Cyclin A/CDK2 complex that is seen during the S phase of the cell cycle also had a consistent expression pattern of the same HALO low and high points for the untreated ALVA-31. The protein p57 had similar expression patterns to that of Cyclin E, where they would interact in the late G1 phase. Also similar were expression patterns of p57 with CDK4, which interact during the G1 phase of the cell cycle. The apoptosis protein c-JUN had a similar pattern to p57, CDK4, and Cyclin E. The proliferation marker PCNA correlated with Cyclin B1 showing a low of HALO 3, and a high of HALO 13.

Table 3.4 ALVA-31: Untreated Expression Points

ALVA-31 UNTREATED		
Apoptosis	Low	High
PCNA	3	13
c-JUN	23	7
KIP	Low	High
p21	23	20
p27	23	13
p57	23	7
Cell Cycle	Low	High
G1 Phase		
Cyclin D1	10	13
CDK2	17	13
CDK4	23	7
Late G1Phase	Low	High
Cyclin E	23	7
CDK2	17	13
S Phase	Low	High
Cyclin A	17	13
CDK2	17	13
G2/M Phase	Low	High
Cyclin A	10	17
Cyclin B1	3	13
CDK1	17	13

Table 3.5 ALVA-31: Selenium Treated Expression Points

ALVA-31 TREATED				
Apoptosis	Low	High	Mesor	Amp.
PCNA	3	20	30.4	25.2
c-JUN	3	17	64	39
KIP	Low	High	Mesor	Amp.
p21	13	10	See	Graph
p27	23	3	See	Graph
p57	10	23	See	Graph
Cell Cycle	Low	High		
G1 Phase				
Cyclin D1	3	10	25.6	12.3
CDK2	N/A	N/A	N/A	N/A
CDK4	N/A	N/A	N/A	N/A
Late G1 Phase	Low	High		
Cyclin E	23	13	20.5	31.3
CDK2	N/A	N/A	N/A	N/A
S Phase	Low	High		
Cyclin A	20	13	63.2	20
CDK2	N/A	N/A	N/A	N/A
G2/M Phase	Low	High		
Cyclin A	20	13	See	Graph
Cyclin B1	20	3	75	8.4
CDK1	13	17	63.8	4.5

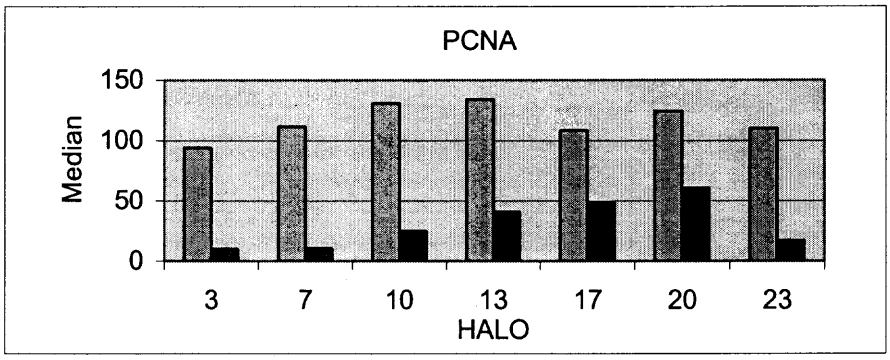

Figure 3.13 ALVA-31 Median Graph of Apoptosis Proteins (1 of 2).

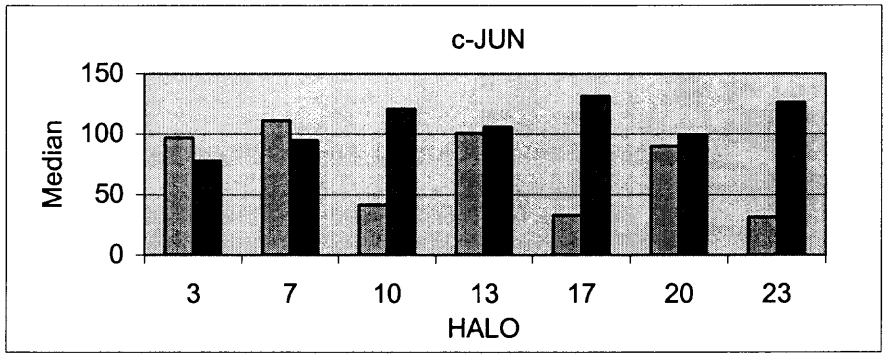

Figure 3.13 ALVA-31 Median Graph of Apoptosis Proteins (2 of 2).

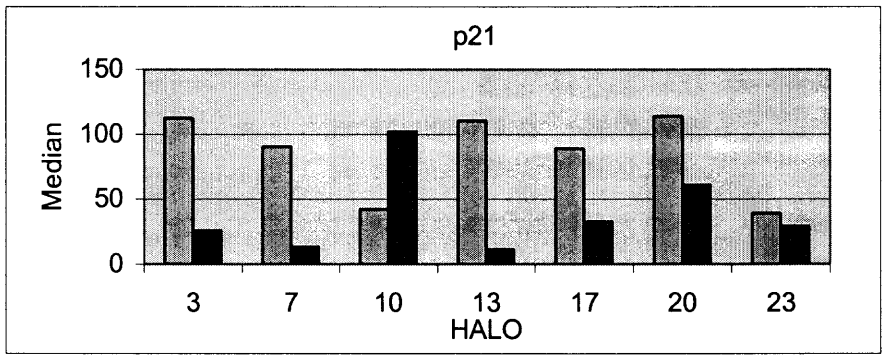

Figure 3.14 ALVA-31 Median Graph of KIP'S (1 of 3).

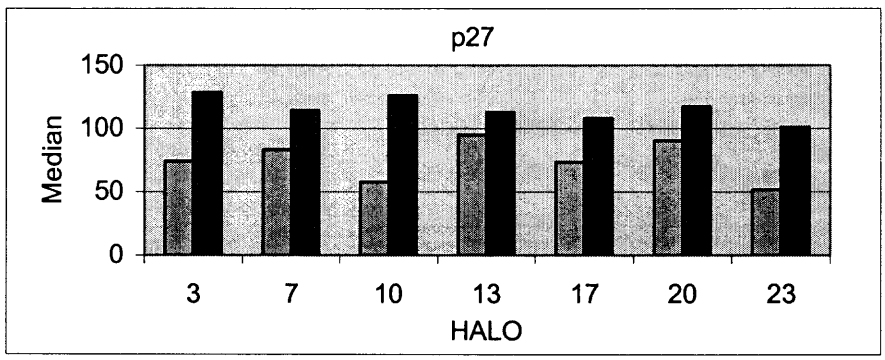

Figure 3.14 ALVA-31 Median Graph of KIP'S (2 of 3).

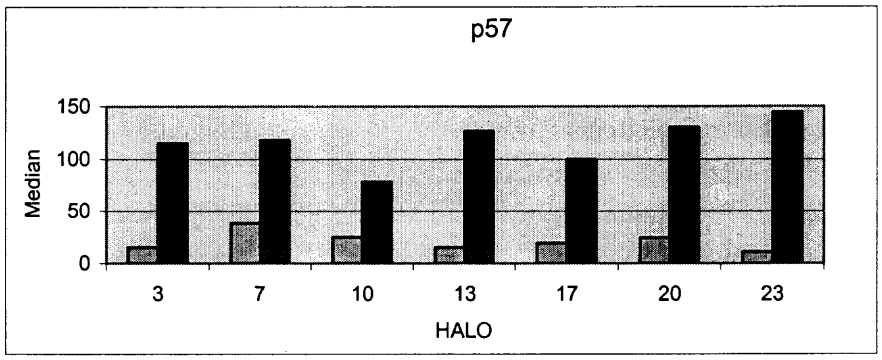

Figure 3.14 ALVA-31 Median Graph of KIP'S (3 of 3).

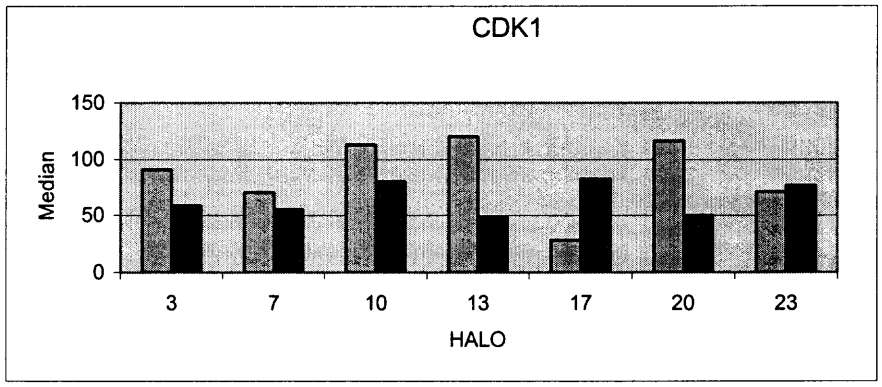

Figure 3.15 ALVA-31 Median Graph of CDK's.

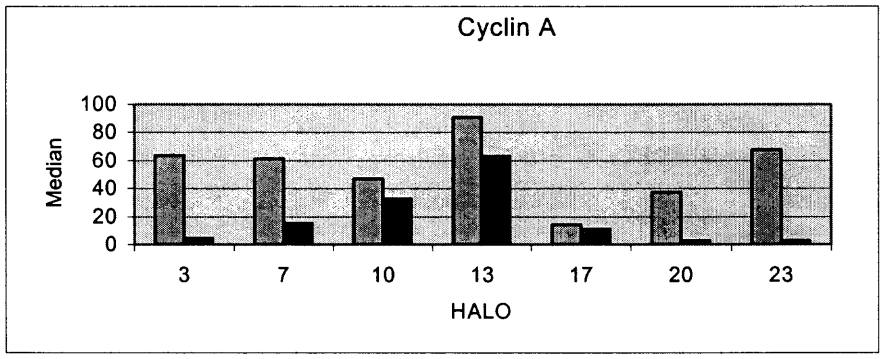

Figure 3.16 ALVA-31 Median Graph of Cyclins (1 of 4).

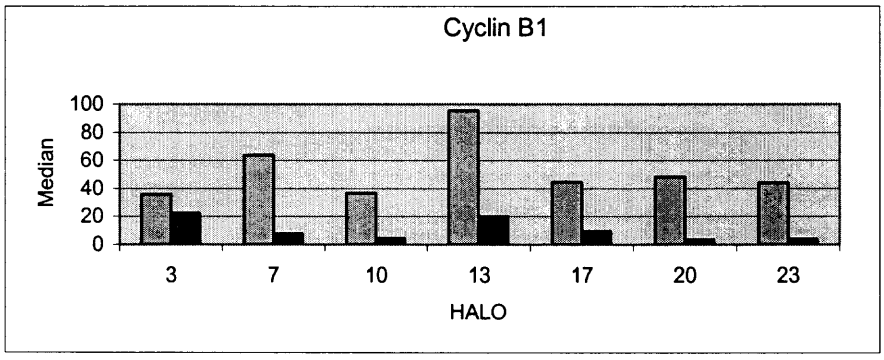

Figure 3.16 ALVA-31 Median Graph of Cyclins (2 of 4).

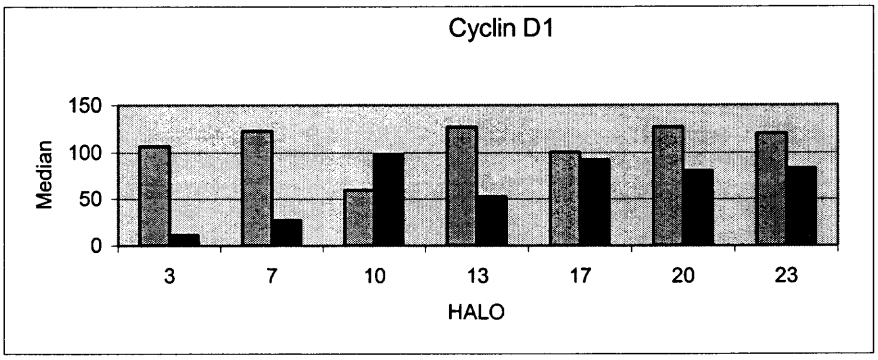

Figure 3.16 ALVA-31 Median Graph of Cyclins (3 of 4).

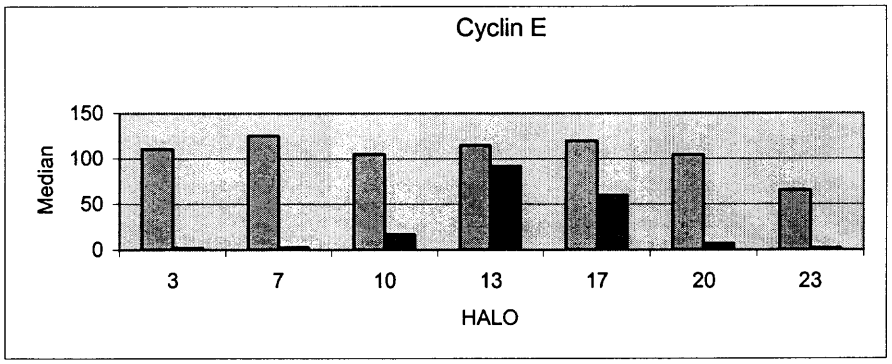

Figure 3.16 ALVA-31 Median Graph of Cyclins (4 of 4).

The KIP'S p21, p27 and p57 were plotted for ALVA-31. Proteins p27 and p57 had similar expression patterns where the expression in treated tumor was higher than in untreated ALVA-31 tumors, while p21 had higher expression in the untreated tumor blots, except for HALO 10 where the treated tumor expression is higher. This is also the highest point of expression for p21.

For the treated ALVA-31 tumors, there was not a consistent pattern between the low and high points of expression between each protein marker. There was a consistency however with the low points of the treated samples PCNA, c-JUN, p27, Cyclin D1 and Cyclin E in the untreated samples of ALVA-31. The high point of Cyclin A untreated and treated correlated.

Expression levels FOR WHAT is higher in kidney and lung than in both treated and untreated tumors, but does not show any significant circadian rhythm. For the KIP'S (p27 and p57) it seemed that the normal tissue was very close to the treated samples.

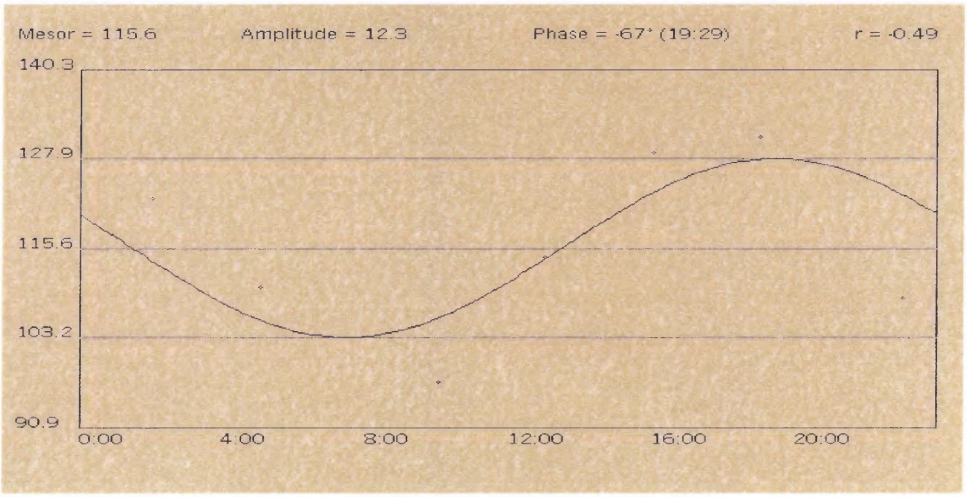

Figure 3.17 ALVA-31 untreated COSINOR using PCNA

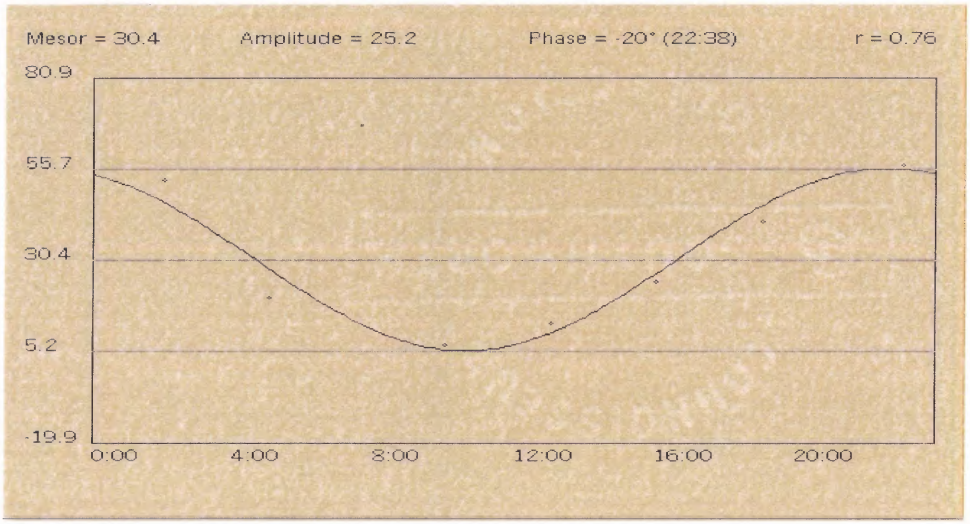

Figure 3.18 ALVA-31 treated COSINOR using PCNA

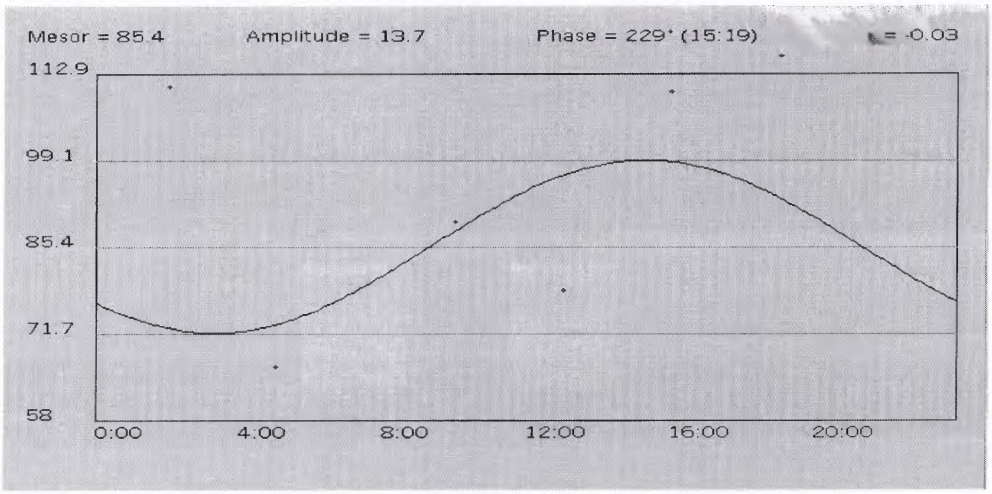

Figure 3.19 ALVA-31 untreated COSINOR using CDK1

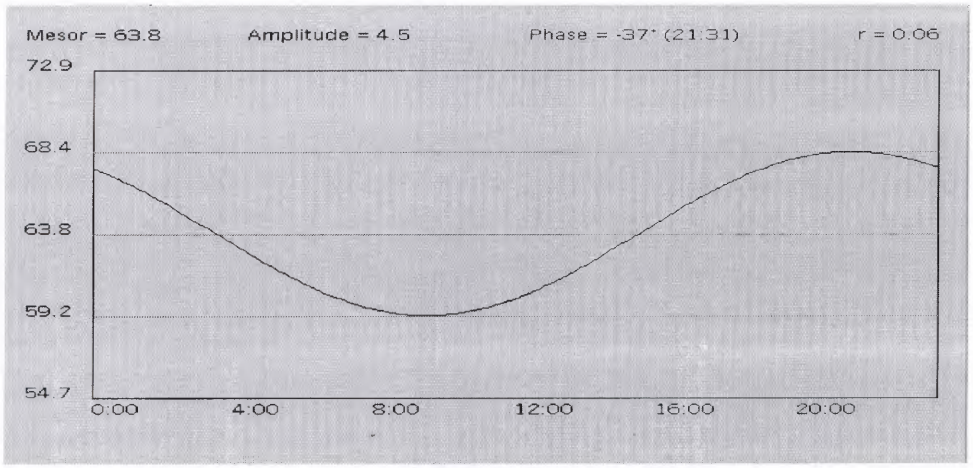

Figure 3.20 ALVA-31 treated COSINOR using CDK1

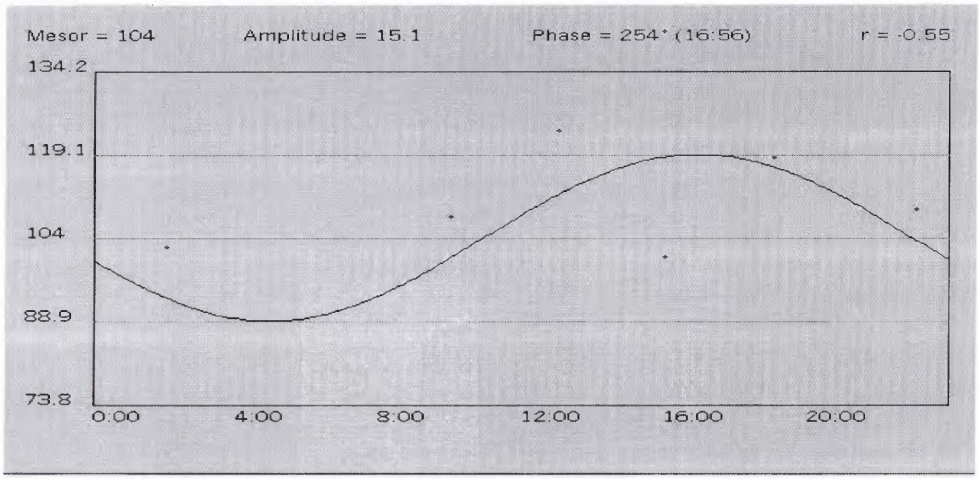

Figure 3.21 ALVA-31 untreated COSINOR using Cyclin E

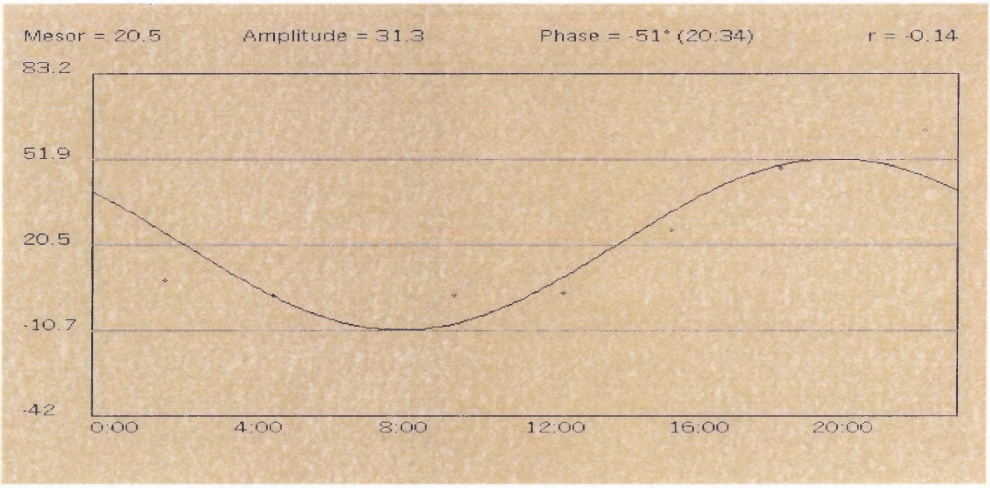

Figure 3.22 ALVA-31 treated COSINOR using Cyclin E

3.5 PC-3 Analysis

The same data (amplitude, mesor, acrophase and low point) were determined from the data and the graphs (See Tables 3.6 and 3.7). For the PC-3 analysis the G1 phase proteins are expressed and had an acrophase in the early HALO's (3, 7 and 10), the Late G1 and S phase proteins in the middle HALO's (10, 13 and 17) and the G2/M phase proteins in the later HALO's (17, 20 and 23). The amplitude and mesor of the proteins that were related in the same cycle exhibited similar values. The PCNA and Cyclin B1 acrophase during HALO 3, but both should be expressed during a later HALO. This discrepancy may be due to problems with the immunoblots, such as uneven drying of the samples (See Figures 3.25-3.27).

Table 3.6 PC-3: Untreated Expression Points

PC-3 UNTREATED				
Apoptosis	Low	High	Mesor	Amp.
PCNA	23	3	32.37	32.21
c-JUN	10	13	75.72	14.42
KIP	Low	High	Mesor	Amp.
p21	23	3	32.15	26.16
p27	10	3	72.52	17.91
p57	10	3	60.67	22.75
Cell Cycle	Low	High	Mesor	Amp.
G1 Phase				
Cyclin D1	20	3	35.44	28.22
CDK2	10	13	46.41	14.45
CDK4	23	3	43.19	25.83
Late G1 Phase				
Cyclin E	3	13	35.14	11.25
CDK2	10	13	46.41	14.45
S Phase				
Cyclin A	10	17	36.24	19.05
CDK2	10	20	46.41	12.76
G2/M Phase				
Cyclin A	10	17	36.24	19.05
Cyclin B1	23	3	48.98	59.77
CDK1	23	13	85.36	40.75

Table 3.7 PC-3: Selenium Treated Expression Points

PC-3 TREATED				
Apoptosis	Low	High	Mesor	Amp.
PCNA	13	23		
c-JUN	13	23	65.47	33.24
KIP	Low	High	Mesor	
p21	13	10	75.33	20.58
p27	13	17	51.68	37.71
p57	13	10	50.53	34.49
Cell Cycle	Low	High		
G1 Phase				
Cyclin D1	13	10	70.51	27.18
CDK2	13	10	51.11	22.71
CDK4	13	10	72.19	32.57
Late G1 Phase				
Cyclin E	13	10	61.46	29.87
CDK2	13	10	51.11	22.71
S Phase				
Cyclin A	13	10	65.03	26.3
CDK2	13	10	51.11	22.71
G2/M Phase				
Cyclin A	13	10	65.03	26.3
Cyclin B1	13	10	46.19	41.49
CDK1	13	23	36.24	34.13

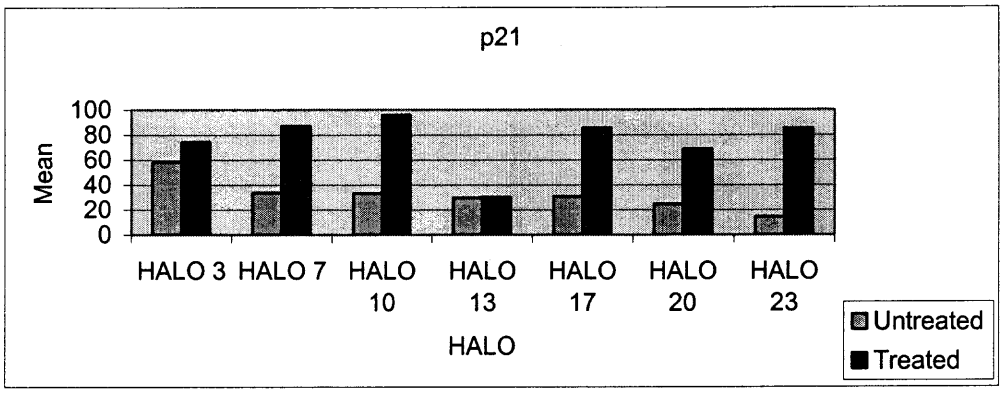

Figure 3.23 PC-3 Mean Graph of KIP's.

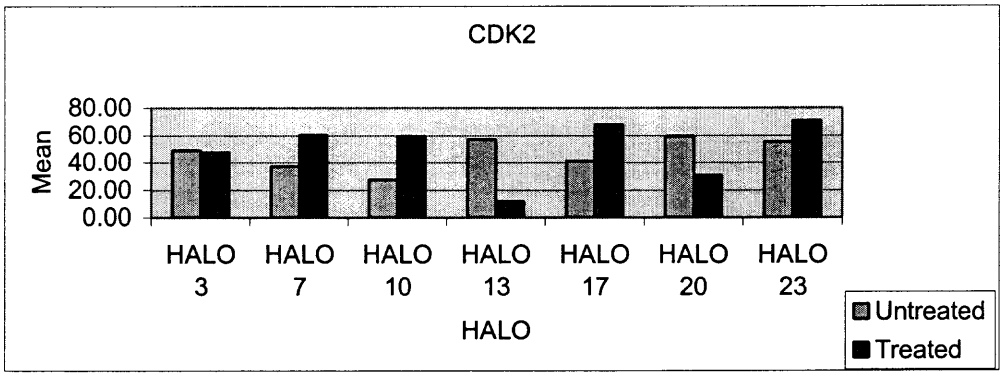

Figure 3.24 PC-3 Mean Graph of CDK's (1 of 2).

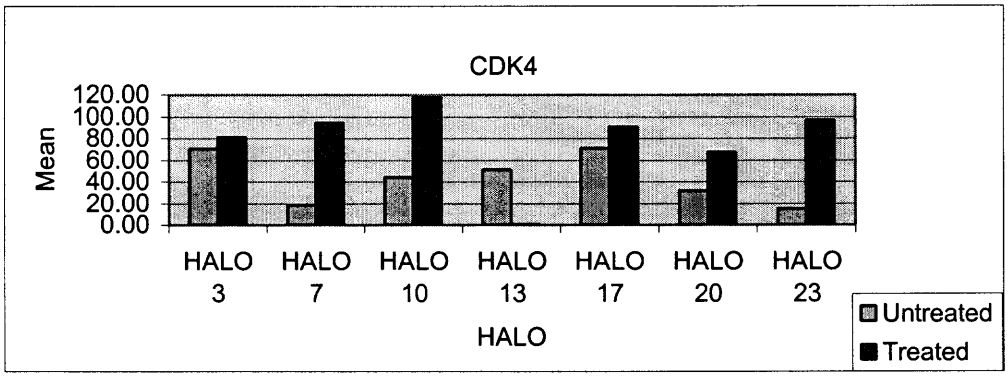

Figure 3.24 PC-3 Mean Graph of CDK's (2 of 2).

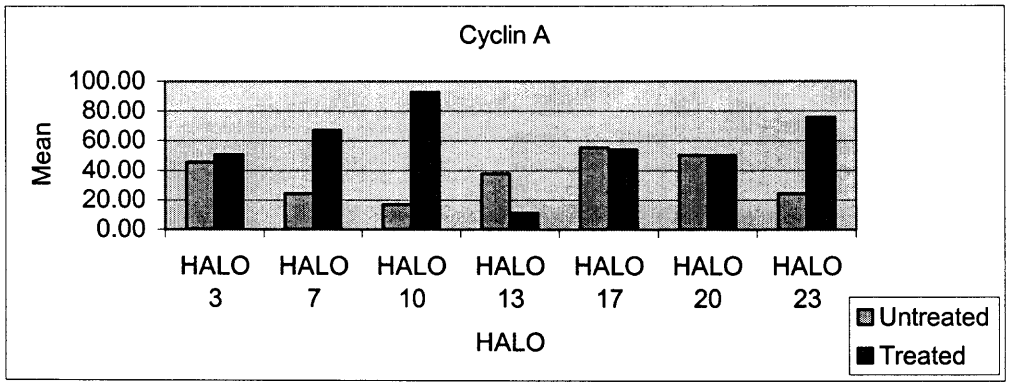

Figure 3.25 PC-3 Mean Graph of Cyclin's (1 of 3).

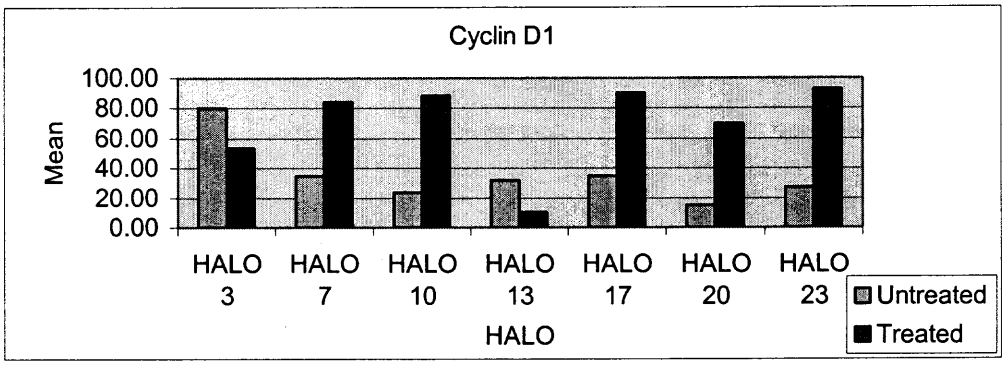

Figure 3.25 PC-3 Mean Graph of Cyclin's (2 of 3).

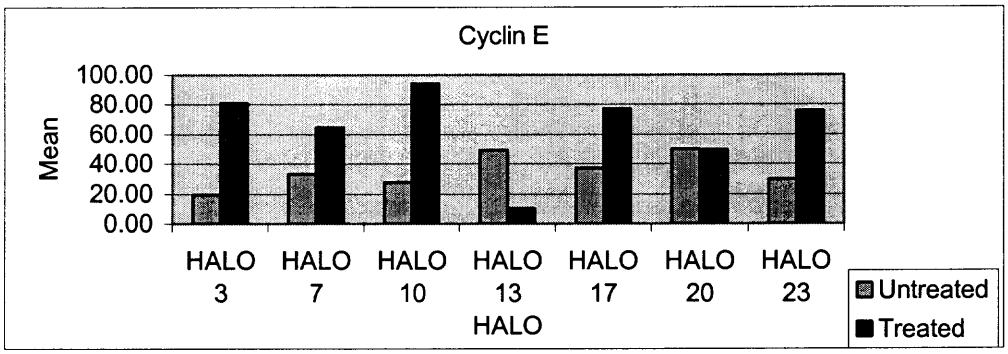

Figure 3.25 PC-3 Mean Graph of Cyclin's (3 of 3).

For PC-3 tumors there seemed to be a correlation of untreated tumors with low expression points of HALO 10 and 23 (4:00 PM and 5:00 AM respectively) for most proteins. This shows a diurnal cyclic pattern for every 12 hours in the untreated tumors. The high points of expression for untreated PC-3 seemed to be HALO 3 and 13 (10:00 AM and 7:00 PM). For sodium selenite treated PC-3, tumors showed that every protein was expressed at HALO 7 (1:00 PM). The highest expression in the treated PC-3 tumors, for the apoptosis proteins were at HALO 23 (5:00 AM) and the cell cycle proteins were uniformly expressed at HALO 10 (4:00 pm) with the exception of CDK1 (HALO23).

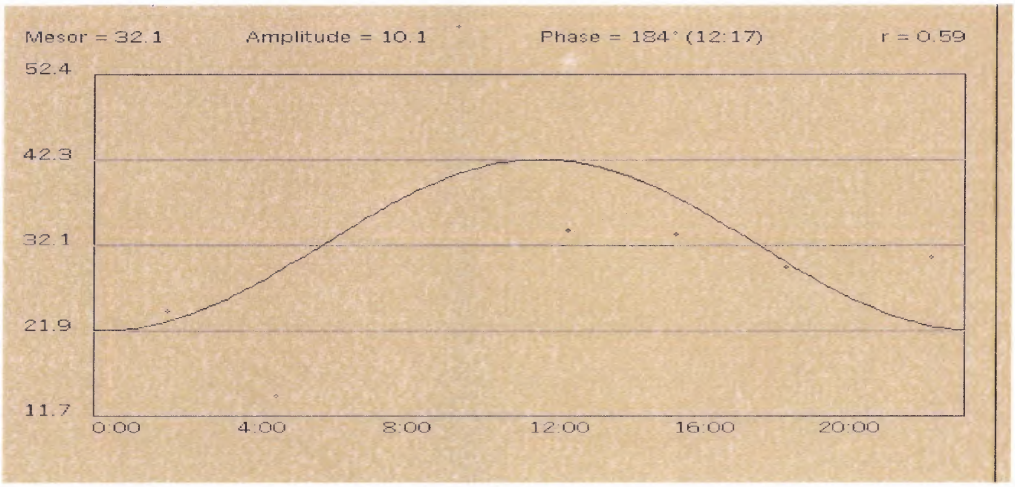

Figure 3.26 PC-3 untreated COSINOR using p21.

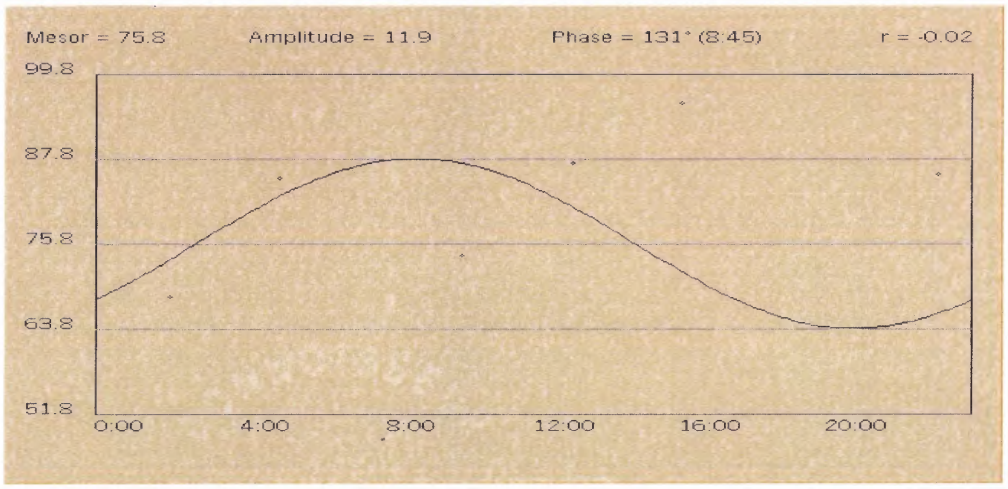

Figure 3.27 PC-3 treated COSINOR using p21.

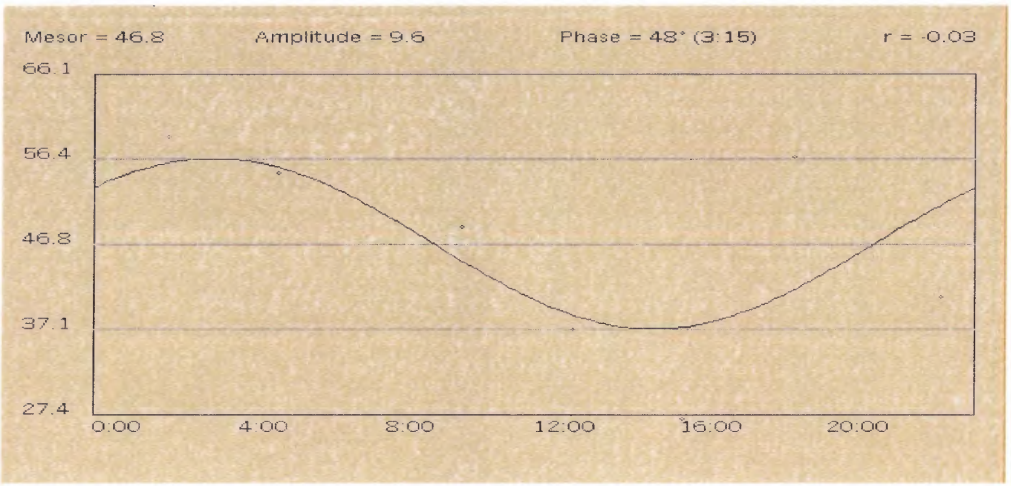

Figure 3.28 PC-3 untreated COSINOR using CDK2.

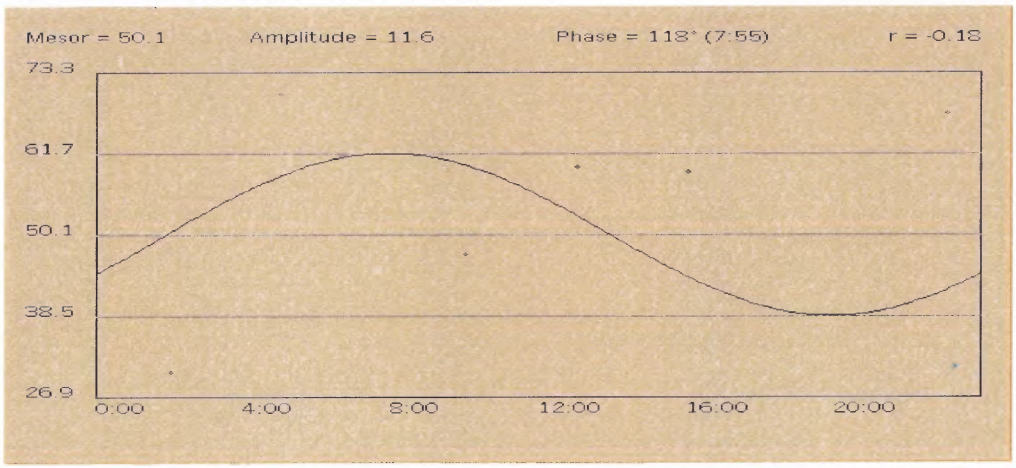

Figure 3.29 PC-3 treated COSINOR using CDK2.

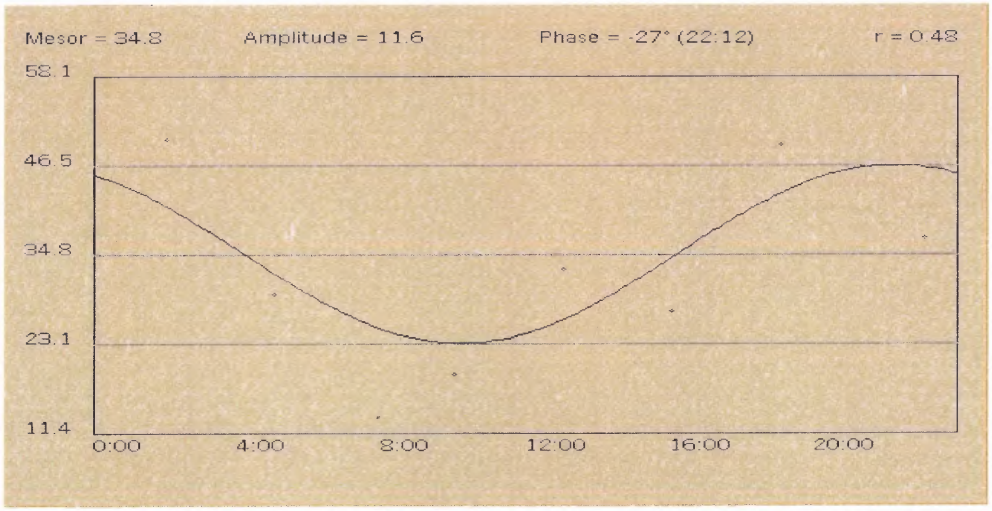

Figure 3.30 PC-3 untreated COSINOR using Cyclin E.

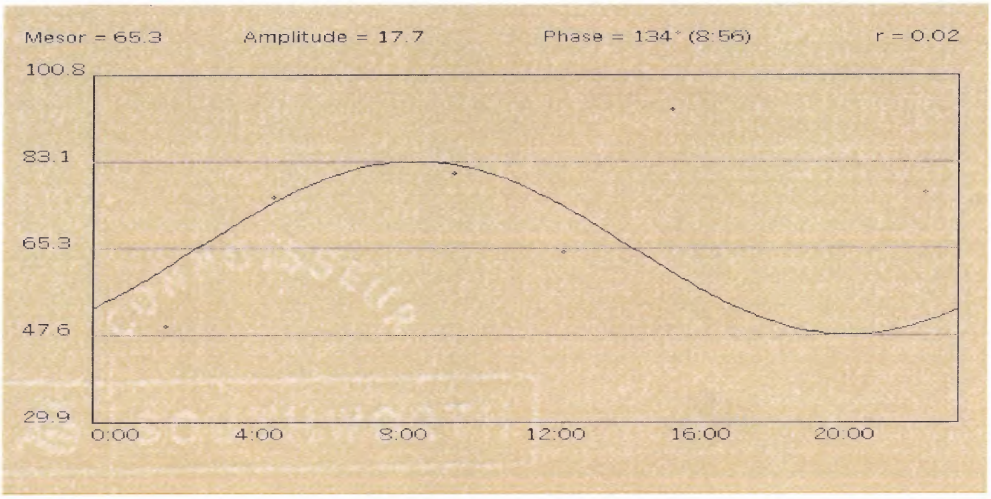

Figure 3.31 PC-3 treated COSINOR using Cyclin E.

CHAPTER 4

DISCUSSION

Identification of tumor expression based on circadian rhythms can be advantageous in the field of oncology. In general, there are biochemical effects not shown that can alter the clinical trial outcome. Multiple genetic changes may result in activating oncogenes, increasing expression of growth factors, and losing function of various genes such as tumor suppressors. The interaction between the tumor cell and host is lost; therefore researchers need as much information as possible to lead to a better understanding of tumor behavior in order to develop accurate therapeutics. Even if this information is provided, two patients with similar tumors and diagnosis may respond differently to the same therapeutic. Studies focused on identifying all properties (size, life cycle, proliferation patterns, ect) of tumors, and in differentiation can result in a formulation of a tumor classification system which can better diagnose and treat patients with cancer. This will guide treatment to derive methods that are more targeted to the individual and the administration of chronotherapeutics.

There are many ways in which chronotherapy may be beneficial. The circadian timing of surgery, anticancer drugs, radiation therapy, and biologic agents can result in improved toxicity profiles, tumor control, and host survival. Using chronobiological principles, clinical trials have confirmed that patients may receive higher levels of chemotherapy and a positive response during this administration (Hrushesky et al., 1993). In support of these results, Grundschober found that 2% (85 genes) of all expressed genes followed a circadian pattern, suggesting a direct link between circadian rhythm and cell

cycle. Bjarnason conducted further studies to relate significant variation of circadian rhythms to high points of expression. For example, p53 expressed in the Late G1 phase (10:56 h), Cyclin E expressed between G1/S phase (14:59 h). In comparison to Bjarnason's studies, the result of this study showed supporting evidence with Cyclin E expression at (13:00 h) for ALVA-31 untreated tumors and (16:00 h) for PC-3 tumors treated with selenium. Furthest results were (19:00 h) for ALVA-31 treated with selenium along with PC-3 tumors. For Bjarnason's study, Cyclin A was expressed in G2 (16:09 h). In comparison, this study found that Cyclin A expressed at a similar time (16:00 h) in PC-3 tumors treated with selenium. Cyclin A had lowest expression at (16:00 h) for ALVA-31 tumors. Both ALVA-31 treated with selenium and PC-3 tumors showed the furthest relation with high points of expression at (19:00 h). Cyclin B in Bjarnason's study was expressed in M (21:13 h). This time frame is between HALO 13 and HALO 17 of this study. The ALVA-31 tumors showed a correlation to this with expression points at (19:00 h). The expression of PC-3 treated with selenium was at (16:00 h). Values that did not correlate with Bjarnason were ALVA-31 treated with Selenium and PC-3 tumors which both expressed at (11:00 h).

There were general differences between the two untreated prostate tumor xenografts ALVA-31 and PC-3, such as the untreated ALVA-31 being higher than the treated. The reverse was true for PC-3 tumors. The apoptosis proteins PCNA and c-JUN showed similar results regarding ALVA-31 treated vs. untreated tumors. The untreated expression of PCNA was higher and the reverse was true for c-JUN suggesting that treatment decreased tumor proliferation and increased apoptosis at all HALOs. The ANOVA can be thought of as an extension of the t-Test to an arbitrary number of factors

and levels. It can also be thought of as a linear regression model whose independent variables are restricted to a discrete set.

From the studies with both ALVA-31 and PC-3, selenium in the sodium selenite form was shown to have inhibitory effects on cell proliferation. With the ALVA-31 samples, all 3 KIPs up-regulated at HALO 10 for selenium treated tumor samples. This might lead one to postulate that HALO 10 dosing with selenium would give maximal therapeutic effects. In an initial therapy study, HALO 10 and 17 dosing gave the best responses. Results were very consistent between treated and untreated tumors; therefore complex information was not relevant. From the data, selenium showed to have inhibitory effects on the cell cycle, while the untreated tumor cells did not have as much of an effect in PC-3 tumors. This could have led to the inference that the untreated tumors kept proliferating without these inhibitory effects. Exceptions to the treatment effects on expression were the KIP's and c-JUN for ALVA-31 since they reflect inhibitory control of tumor growth. For the PC-3 tumors, a majority of the selenium treatments at HALO 13 were exceptions to the selenium trend and showed lower levels of expression. These results need to be compared with other studies carried out with sodium selenite and prostate cancer to be compared. The next step would be to go through trials mice with different phases of time, and testing with other types of normal tissue (GI tract, marrow, ect). In humans, one could implement Phase I chrono-dose testing to identify properties and adverse effects in humans. Additional studies could be carried out to determine whether the sodium selenite prevents the occurrence of prostate cancer in various animal models

The main difficulty of this study was to obtain consistent patterns of immunoblot data. From repeating the blots, trends developed among the tumor lines, the sodium selenite treated blots, and the organs. Each group had different properties and therefore the immunoblot process changed with the handling of each group. Between the ANOVA and COSINOR methods, the COSINOR method proved to show more accurate results in plotting while both displayed the Mean, Mesor, Amplitude and Acrophase of the data. Also, the protein PCNA was used for the ALVA-31 tumor lines and tested with treated vs. untreated, while the PC-3 tumor lines were tested with the PJNK protein. This led to inconsistency in data because although they were both apoptosis regulating proteins, they can not be used in a direct comparison. Another complication was the inflexibility of the COSINOR program which did not allow adjustments of the axis, and therefore did not show consistency in displaying the results. Problems that lie ahead would be to find a standard to quantify these results. Testing selenium in conjunction with new treatments that are becoming available could be a next step towards continuing the studies and effects of selenium as a supplementary therapy to a primary therapeutic.

New treatments are becoming available or are currently undergoing clinical trials in various pharmaceutical discovery companies. For Example, Velcade™, is a new agent currently in clinical trials, and is aimed at building BAX levels to inhibit bcl-2 for the cell to ultimately undergoes apoptosis (NCI 2003). Another agent in clinical trials that induces apoptosis is Genasense™. Androgen suppression is a therapy which may reduce levels of male hormones. Adjunct use of these forthcoming or existing treatments with selenium treatment may impact prostate cancers or slow their growth.

Time related dosing can result in improved quality of life. This study examined the effect of the treatment selenium on two prostate tumor xenografts, and compared the untreated tumor to the treated tumors, as well as normal tissue of lung and kidney. The normal tissue comparison did not show significant differences to be notable. Further studies could be carried out in order to try and determine significant differences. A high level of expression could infer continuous presence of the proteins in both lung and kidney. For the ALVA-31 tumor models, there were significant results in comparison of all Cyclin's against Apoptosis proteins. The PC-3 tumor models all consistently showed a higher expression of treated tumors when compared to untreated. Particularly, HALO 10 as the highest level of expression for sodium selenite treated tumors. The more our understanding of cycles and their involvement of biological processes such as cell and apoptosis, the more effective chemotherapeutic treatments may become, to ultimately improve clinical efficacy and reach a level of acceptable clinical toxicity.

REFERENCES

Alisauskas R, Flynn M, Goldenberg D, Blumenthal R. Chronobiological principles associated with preclinical IL-12-based therapy. Proc. Amer. Assoc. Cancer Res. 1999;40;abstract 517:78.

American Association for Cancer Research
Retrieved August 18th, 2003 from the World Wide Web:
http://cancerres.aacrjournals.org/misc/terms.shtml.

American Cancer Society. Cancer Facts & Figures2001; Prostate.
Retrieved July 8th, 2003 from the World Wide Web:
http://www.prostateinfo.com/patient/treatment/other.asp.

Bjarnason G, Jordan R, Sothern R. Circadian Variation in the Expression of Cell Cycle Proteins in Human Oral Epithelium. Journal of Pathology 1999;154(2):613-622.

Blumenthal R, Ochakovskaya R, Osorio L, Ying Z, Goldenberg D. Regulation of tumour drug delivery by blood flow chronobiology. Eur. J. Cancer 2001;36:1876-1884.

Blumenthal R, Sharkey R, Haywood L, Behr T, Goldenberg DM. Application of cytokine intervention for improved radio-antibody dose delivery. Int. J. Cancer 1997;72(1):166-173.

CDC: Center for Disease Control.
Retrieved August 18th ,2003 from the World Wide Web:
http://www.cdc.gov/genomics.

Cdks Mediate Cell Cycle Progression
Retrieved August 18th ,2003 from the World Wide Web:
http://cpmcnet.columbia.edu/dept/eukaryotic/cobriniknotes1.pdf.

Clark L, Dalkin B, Krongrad A. Decreased incidence of prostate cancer with selenium supplementation: results of a double-blind cancer prevention trial. Br J Urol 1998;81:730–734.

Combs G, Jr., Clark L, Turnbull B. Reduction of cancer risk with an oral supplement of Selenium. Biomed Environ Sci 1997;10:227-34.

Combs G, Jr and Gray W. Chemopreventive agents: Selenium. Pharmacol Ther 1998;79:179-92.

Davis. Research Sheds New Light On Why Some Prostate Cancers Become Untreatable. Retrieved July 16th ,2003 from the World Wide Web: http://www.ucdmc.ucdavis.edu/news/untreatable_prostatecancer.html.

Dong Y, Zhang H, Hawthorn L, Ganther H, Ip C. Delineation of the Molecular Basis for Selenium-induced Growth Arrest in Human Prostate Cancer Cells by Oligonucleotide Array. Cancer Research 2003 Jan;63:52-59.

Duffield G, Best J, Meurers B, Bittner A, Loros J, Dunlap J. Circadian Programs of Transcriptional Activation, Signaling, and Protein Turnover Revealed by Microarray Analysis of Mammalian Cells. Current Biology 2002 Apr 2;12:551-557.

Focan C. Marker rhythms for cancer chronotherapy. From laboratory animals to human beings. In Vivo 1995;9(4);283-98.

Garland M, Morris J, Stampfer M, Colditz G, Spate V, Baskett C, Rosner B, Speier F, Willett W, Hunter D. Prospective study of toenail Selenium levels and cancer among women. J Natl Cancer Inst 1995;87:497-505.

Grundschober C, Delaunay F, Pulhofer A, Triqueneaux G, Laudet V, Bartfai T, Nef P. Circadian Regulation of Diverse Gene Products Revealed by mRNA Expression Profiling of Synchronized Fibroblasts. JBC 2001 Dec 14;276:46751-46758.

Harnessing Apoptosis to Destroy Cancer Cells
Retrieved August 18th, 2003 from the World Wide Web: www.eur.nl/fgg/pathol/research/ trapman/androgen_receptor.html.

Harris, A. L., Nicholson, S., Sainsbury, R., Wright, C., & Farndon, J. J. Natl. Cancer Inst. Monogr. 1992;11:181–187.

Healthlink. Sleep and Circadian Rhythms. Medical College of Wisconsin 1999; Retrieved June 6th, 2003 from the World Wide Web: http://healthlink.mcw.edu/article/922567322.html.

Healthnotes. Prostate Cancer 2002;
Retrieved September 15th, 2003 from the World Wide Web: http://www.hollandandbarrett.com/healthnotes/Concern/Cancer_Prostate.htm#Conventional-Options.

Hercberg S, Galan P, Preziosi P, Roussel AM, Arnaud J, Richard MJ, Malvy D, Paul-Dauphin A, Briancon S, Favier A. Background and rationale behind the SU.VI.MAX Study, a prevention trial using nutritional doses of a combination of antioxidant vitamins and minerals to reduce cardiovascular diseases and cancers. Supplementation en Vitamins et Mineraux AntiXydants Study. Int J Vitam Nutr Res 1998;68:3-20.

Hrushesky W, Bjarnason G. Circadian cancer therapy. J.Clin. Oncol. 1993;11(7);1403-1417.

Ka Yin K, Mien-Chie H. A novel splice variant of *HER2* with increased transformation activity. Molecular Carcinogenesis 1998;23(2):62-68.

Kimball J. The Cell Cycle. 2003;
Retrieved June 8th ,2003 from the World Wide Web:
http://www.users.rcn.com/jkimball.ma.ultranet/ BiologyPages/C/CellCycle.html.

Kobayashi M, Wood PA, Hrushesky WJ. Circadian chemotherapy for gynecological and genitourinary cancers. Chronobiol. Int. 2002 Jan;19(1):237-51.

Kwong, KY, Hung, MC. A novel splice variant of HER2 with increased transformation activity Mol. Carcinog. 1998;23:62-68.

Leewansangtong S, Crawford E. Maximal androgen withdrawal for prostate cancer therapy: current status and future potential. Endocrine-Related Cancer 1998; 5: 325-339.

Levi F. Chronopharmacology and chronotherapy of cancers. Path. Biol. 1996;44(7):631-644.

Meyer, J.-P.; Gillatt, D. A. Prostate Cancer & Prostatic Diseases 2002;5(1):3, 13.

Mormont M, Levi F. Circadian –system alterations during cancer processes; a review. Int. J. Cancer 1997;70(2):241-247.

Mormont MC, Levi F. Cancer chronotherapy: principles, applications, and perspectives. Cancer 2003 Jan 1;97(1):155-69.

National Research Council. Food and Nutrition Board. Recommended Dietary Allowances. 10th ed. Washington, DC: National Academy Press, 1989.

NCI PRG Current Status in the field 2003;
Retrieved August 18th ,2003 from the World Wide Web:
http://prg.nci.nih.gov/prostate/prgmodels.html.

NCI The Nation's Investment in Cancer Research for Fiscal Year 2004. 2003; Retrieved August 18th ,2003 from the World Wide Web: http://plan.cancer.gov/discovery/apoptosis.htm.

Pienta K, Sandler H, Shah N, Sanda M. Cancer Management: A Multidisciplinary Approach: Medical, Surgical and Radiation Oncology, Chapter 17, Prostate Cancer 2002; Retrieved September 4th ,2003 from the World Wide Web: http://www.cancer.med.umich.edu/prostcan/prosintro.htm.

Richardson G, Tate B. Hormonal and Pharmacological Manipulation of the Circadian Clock: Recent Developments and Future Strategies. Sleep 2000; 23 Suppl 3: S77-85.

Rokhlin O, Bishop G, Hostager B, Waldschmidt T, Sidorenko S, Pavloff N, Kiefer M, Umansky S, Glover R, Cohen M. Fas-mediated Apoptosis in Human Prostatic Carcinoma Cell Lines. Cancer Research 1997 May;(57):1758-1768.

Russo AA, Jeffrey PD, Patten AK, Massague J, Pavletich NP. Crystal structure of the p27Kip1 Cyclin-dependent-kinase inhibitor bound to the Cyclin A-CDK2 complex. Nature 1996 Jul 25;382(6589):325-31.

Russo MW, Murray SC, Wurzelmann JI, Woosley JT, Sandler RS. Plasma Selenium levels and the risk of colorectal adenomas. Nutr Cancer 1997;28:125-9.

Sherr, CJ. Cancer Cell Cycles: Cyclin regulation. Science 1996;274:1672-1677.

Sielecki, TM, et al. Cyclin-Dependent kinase inhibitors: Useful targets in cell cycle regulation. J. Med. Chem. 2000;43:1-18.

Shah M, Schwartz G. Cell cycle-Mediated Drug Resistance: An Emerging Concept in Cancer Therapy. Clinical Cancer Research 2001 Aug;7:2168-2181.

The Biology Project. The University of Arizona Thursday, April 24, 1997; Retrieved August 18th ,2003 from the World Wide Web: http://www.biology.arizona.edu.

UCLA.
Retrieved August 18th ,2003 from the World Wide Web: http://www.bol.ucla.edu/~tolu.

Weissman K. Life and Cell Death. Chemistry in Britain 2003 Aug; 10-22.

Ziada AM, Crawford ED. Advanced prostate cancer. Prostate Cancer Prostatic Dis. 1999 Jan;2(S1):21-26.